Travel Behaviour and Society 43 (2026) 101232

Contents lists available at ScienceDirect

Travel Behaviour and Society

journal homepage: www.elsevier.com/locate/tbs

Spatial and operational interventions for healthy cruise ship design using agent-based modelling

Jiayu Pan [a,*], Leonel Aguilar [b], Michal Gath-Morad [a], Ronita Bardhan [a], Koen Steemers [a]

[a] Department of Architecture, University of Cambridge, Cambridge CB2 1PX, United Kingdom
[b] Chair of Cognitive Science, ETH Zürich, Zürich, Switzerland

ARTICLE INFO

Keywords:
Cruise ship
Health emergency
Spatial design
Operational intervention
Deck plan
Passive mitigation strategies

ABSTRACT

Cruise ship environments have been identified as high-risk settings for communicable disease outbreaks. The severe COVID-19 outbreaks aboard several cruise ships have further intensified concerns about transmission in these confined, densely populated environments. Although some behavioural interventions have been studied, the influence of spatial and operational design on transmission risk remains under explored.

To address this gap, this study applies agent-based modelling (ABM) to simulate passenger movement patterns on mixed-use cruise ship decks as a surrogate for infection transmission. By modelling individual movement behaviours and collisions (close-contact exposure) within the mixed-use decks, the ABM approach supports the development of spatial design and operational strategies that can reduce transmission risk and improve the efficiency and healthiness of onboard circulation. We conducted verification and parametric tests to assess model performance and designed three experiments to evaluate the effects of varying occupancy levels, infection prevalence, spatial layouts and access restriction strategies with 1181 simulation runs, the simulation results are complemented by spatial analyses of deck plans to inform evidence-based recommendations for safer cruise ship environments.

We identified three key spatial drivers of disease transmission risk on cruise ships. First, higher occupancy density and compact layouts significantly increased close-contact events, as passengers navigated narrow, poorly connected corridors. Second, the effectiveness of quarantine interventions depended not just on their presence but on their spatial placement: centrally located restrictions amplified congestion, while peripheral placement helped alleviate it. Third, simple passive design changes—such as widening corridors or enhancing internal connectivity—reduced movement bottlenecks and collisions, without requiring behavioural adaptation. Together, these findings demonstrate that spatial configuration is not merely a backdrop but a powerful determinant of health resilience in high-occupancy environments.

1. Introduction

Cruise ships are inherently high-risk environments for infectious disease outbreaks due to their densely occupied, enclosed and semi-closed spaces combined with limited onboard health resources and frequent embarkation and disembarkation. These conditions facilitate the rapid transmission of person-to-person, foodborne and waterborne diseases (Golna et al., 2024; Nemhauser and Centers for Disease Control (U.S.), 2023; Zhang et al., 2020). The COVID-19 pandemic highlighted these vulnerabilities, with outbreaks on ships like the *Diamond Princess*, *Ruby Princess* and *Celebrity Apex* demonstrating how confined environments can accelerate infection spread. Passengers and crew exposed to extended periods of quarantine on ships faced high health risks and limited access to medical care, underscoring the critical need for improved health risk management strategies in cruise ship design and operations.

The cruise industry has fully recovered from the major impact of the pandemic, with global passenger volume exceeding pre-pandemic passenger volumes in 2023 by 6 %. Cruise ships are increasingly becoming a popular way of travelling as demonstrated by a growing passenger population and increasing economic impact (Cruise Lines International Association, 2024; J.P. Morgan Research, 2024). However, although the

* Corresponding author at: Department of Architecture, 1-5 Scroope Terrace, Cambridge CB2 1PX, England, United Kingdom.
E-mail address: jp844@cam.ac.uk (J. Pan).

https://doi.org/10.1016/j.tbs.2026.101232
Received 14 July 2025; Received in revised form 23 November 2025; Accepted 2 January 2026
Available online 7 January 2026

threat of COVID has retreated, the vulnerability to onboard disease outbreaks persists. Despite some improvements in awareness, the challenges associated with long-term close contact, complex population flows and insufficient medical infrastructure remain largely unresolved (Zhang et al., 2016). These factors emphasise the urgency to understand cruise ship spatial design and operational measures to better respond to future public health emergencies.

The epidemiology of infectious diseases in enclosed environments like ships has been studied in relation to airborne transmission, contact rates and population density. Yet morphometrics of the enclosed space is mostly used to dictate the ventilation parameters, human aggregation dynamics and mobility outcomes. These in turn impact the success of infection containment interventions. The role of spatial design of enclosed spaces in infection dynamics remains underexplored (Mosleh et al., 2024; Wang et al., 2023). Specifically, the influence of architectural layout, circulation patterns and spatial connectivity on the initial spread of infection and the subsequent efficacy of containment strategies such as quarantine warrants further enquiry. This study addresses this gap by examining how the spatial configuration of ship environments impacts the diffusion of infectious agents and the outcomes of intervention measures. Employing an agent-based modelling (ABM) approach, the study simulates individual movements and interactions within various spatial layouts to assess infection propagation across different activity zones. The study further evaluates the effectiveness of spatially informed quarantining strategies such as zoning, isolation corridors and compartmentalisation in mitigating transmission.

Studies on the built environment during the pandemic have highlighted the significant role of indoor environments in mitigating disease spread. As humans spend the majority of their time indoors, factors such as air quality, surface contamination and physical contact significantly influence transmission risks (Clements et al., 2020). Agent-based modelling (ABM), which can be applied to simulate individual movements and interactions, has proven to be an effective tool for analysing human behaviour in indoor environments. By testing various possible strategies to reduce the frequency of close contacts among individuals, ABM can be used to offer insights about how to limit the spread of communicable diseases in dense, enclosed settings like cruise ships.

This study focuses on leveraging ABM to develop a framework for investigating the operational strategies and spatial design of cruise ships to limit infection transmission. As illustrated in Fig. 1, spatial layouts and operational measures can influence passenger behaviour, particularly movement patterns, which, in turn, affect the collision between passengers and the risk of disease transmission. The applicability of ABM is particularly relevant to cruise ships, where passengers spend considerable time navigating ship decks – especially on sailing days.

The objectives of this study are outlined as follows:

- Develop an agent-based model using *DesignMind* toolkit (Baur et al., 2023) to simulate passenger movement on cruise ship decks, demonstrated through three case studies.
- Analyse the spatial structure of deck plans.
- Validate and verify the agent-based movement simulation with validation and parametric tests.
- Conduct experiments to examine how:
  - o Passenger density affects infection spread risks (Experiment 1).
  - o Operational strategies, like partial corridor quarantines, influence movement behaviour (Experiment 2).
  - o Design layout modifications impact movement patterns (Experiment 3).

In this manuscript, Section 2 reviews the relevant literature about the studies on health in cruise ship environments and the application of ABM in interior environments. Section 3 introduces the method, including a description of the ABM, testing protocols of the model and experimental setup. Section 4 reports the results of the validation and verification tests, and Section 5 showcases the results of the three experiments. Section 6 presents the conclusions and future research.

2. Literature review

2.1. Public health emergencies on cruise ships

Outbreaks of various types of infectious diseases, such as H1N1/Influenza A, norovirus and COVID-19, on cruise ships have been reported regularly (Anagnostopoulos et al., 2025; Bert et al., 2014; Nemhauser and Centers for Disease Control (U.S.), 2023). The frequent stops at international ports expose passengers to local diseases, which can then be incubated on board and facilitate further global disease transmission, highlighting the role of cruise ships in amplifying public health risks. These combined factors call for evidence-based practices and cross-sector collaboration, to prevent and control infectious disease on ships (Anagnostopoulos et al., 2025).

Previous studies have investigated the spread of infectious disease in cruise ships (Bert et al., 2014; Rocklöv et al., 2020; Zhang et al., 2016, 2020), especially during the COVID-19 pandemic outbreak. The outbreaks on cruise ships provide insights for epidemiologists to study the spread of COVID-19 in similar settings, such as nursing homes, hotels and prisons. The case of *Diamond Princess* is widely studied due to its uniqueness (Baraniuk, 2020). Over 3700 people had been quarantined on the ship, and 721 passengers and crews were tested positive (Japan Institute for Health Security, 2020). The estimated R_0 at the beginning was 3.27 and rose to 4.18 and 4.73 including asymptomatic transmission when quarantine started (Huang et al., 2021). A global study found that the proportion of COVID-19 infection on cruise ships is significantly associated with the number of cabins, the number of decks with cabins and passenger-to-space ratio. Enhancing health protection measures is important for restoring customers' trust in cruise ship operations post COVID-19 (Yuen et al., 2021).

In order to restrict the spread of infectious disease in cruise ship, quarantine is a straightforward response in health emergencies. Movement restrictions for symptomatic individuals, especially early self-isolation or full-ship quarantine, proved particularly effective (Codreanu et al., 2021; Srinivasan et al., 2024). Fully closing all dining areas can significantly reduce norovirus transmission, while partial closures may worsen the spread due to crowding (Srinivasan et al., 2024). Mitigation strategies such as wearing masks in public spaces and vaccination can reduce the COVID-19 cases by over 94 % (Mosleh et al., 2024). The use of technological solutions, such as wearable devices, cameras, air purifiers and air quality sensors, to screen for and detect early spread of prevalent communicable diseases on cruise ship, is a possible solution, following the improvements in passengers' awareness and education (Golna et al., 2024; Hao, 2023).

Typically, research on cruise ships also focuses on the evacuation during emergencies (Cotfas et al., 2023; Firdhaus et al., 2023; Yue et al., 2022) and leisure experience and satisfaction of cruisers (Castillo-Manzano and López-Valpuesta, 2018; Ozturk and Gogtas, 2016; Xie et al., 2012). The majority of published work about infectious disease spread on ships emphasises personal protective and behavioural measures for travellers, with comparatively limited attention to environmental or spatial factors (Anagnostopoulos et al., 2025). Research gaps remain in understanding the interior spatial design and related passenger behaviour on cruise ships.

2.2. Agent-based movement simulation in indoor environments

Agent-based movement models have the potential to be applied in testing the design and operation of indoor spaces, by simulating the movement patterns of human agents. This application has been demonstrated in the past research with various ABM tools, showcasing the potential of this emerging field.

In agent-based modelling *'a system is modelled as a collection of autonomous decision-making entities called agents. Each agent individually*

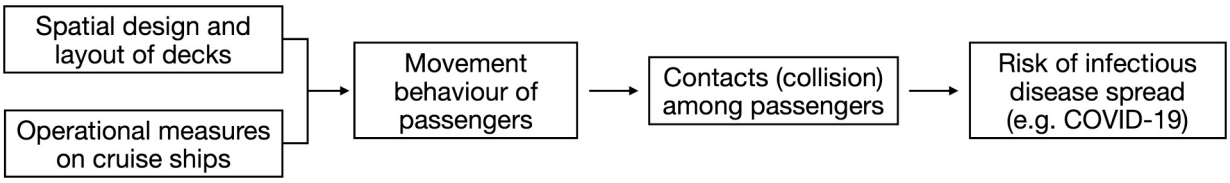

Fig. 1. Key assumption of the study.

assesses its situation and makes decisions on the basis of a set of rules' (Bonabeau, 2002). ABM enables researchers to build, investigate and experiment with models made up of autonomous, heterogeneous agents interacting within a defined environment, to explore and identify the underlying mechanisms that lead to observable patterns (Salgado and Gilbert, 2013).

Architectural design is often seen as a creative problem-solving process that integrates both building and occupant information (Ekholm, 2001). In the field of architectural design, the application of ABM for movement simulation at the level of individual users can examine building-related spatial activities and behaviours, to study the inter-relationship between the physical environment and human behaviour, and subsequently inform the design of spaces (Cheliotis, 2021, 2020; Liu et al., 2014; Stieler et al., 2022). Simulation with ABM generates a large amount of spatial–temporal data to understand how people use spaces (Gath-Morad et al., 2017). The application of ABM simulation in design has been demonstrated in various environments, such as offices (Pan et al., 2021; Schaumann et al., 2020; Tabak et al., 2010; Yu, 2023), hospitals (Gath-Morad et al., 2023; Jia et al., 2023; Schaumann et al., 2017), supermarkets (Antczak et al., 2021; Xu and Chraibi, 2020), university buildings (D'Orazio et al., 2021), airports (Arup, 2024) and rail stations (Castle et al., 2011). The performance of the model is often validated by real world data from field observation, occupancy sensors, VR experiments and interviews with users and experts (Cheliotis, 2020; Morad et al., 2020; Schaumann et al., 2017; Tabak et al., 2010).

Spatial parameters are often combined with ABM to understand and evaluate wayfinding behaviour and space use (Cheliotis, 2020; Neumayr, 2019; Noyman et al., 2024; Torrens, 2015; Yu, 2023). Environmental factors like temperature, acoustics (Schaumann et al., 2020) and indoor air quality (Martinez et al., 2022), spatial factors like building layout, location of equipment and visibility and social factors like social networks and the presence or absence of people, can also be considered and integrated into ABM models (Schaumann et al., 2017). Previous studies and real-world practices have demonstrated that ABM can be used to evaluate different layout configurations, allowing designers to test various scenarios and iterate the design (Hong et al., 2016). The simulation of users' activities and occupancy can also contribute to the analysis and prediction of energy use (Yan et al., 2015). Furthermore, modelling and predicting building-user interactions can contribute to the improvements of occupants' physical comfort, social well-being and satisfaction level (Schaumann et al., 2017).

Some critical or emergency scenarios have highlighted the value of applying simulation ABM tools to evaluate potential outcomes and consequences. In health emergencies like the COVID-19 pandemic, ABMs can bridge building design and infection control, supporting the concept of healthy buildings. The impacts of infection control measures such as social distancing, capacity reduction, access control (Antczak et al., 2021; D'Orazio et al., 2021; Pan et al., 2021; Xu and Chraibi, 2020), shifts between workers, enhanced ventilation (Martinez et al., 2022) and use of masks can be tested (Noakes et al., 2006) and used to inform facility managers, as well as estimate the risk of infectious disease transmission (Antczak et al., 2021; Zhen et al., 2022; Zhou and Koutsopoulos, 2021). For example, ArchABM is an agent-based simulator coupling occupant schedules and ventilation, to predict CO_2 and viral aerosol loads in a research centre (Martinez et al., 2022). Likewise, the VIRIS framework explicitly combines spatial structure, people's movement and airborne transmission physics to predict spatiotemporal infection risk in spaces like courtrooms, care homes or supermarkets (Xue et al., 2024). In evacuation conditions triggered by a fire, an earthquake, or building collapse, with very limited real-world observation and limited capacity for real-world investigations (Torrens, 2015, 2012), ABM has been used to model the behaviour of occupants during emergencies (Cotfas et al., 2023; Kasereka et al., 2018; Ren et al., 2009), providing insights into evacuation times, the effectiveness of signage, the impact of different evacuation strategies and the number of successful evacuations.

Transmission within enclosed environments has been modelled using distinct but complementary approaches (Christakis and Drikakis, 2024; Sofos et al., 2025). Airborne exposure and aerosol transport are commonly analysed using Wells–Riley formulations and Computational Fluid Dynamics (CFD) to estimate pathogen concentrations and inhalation risk as a function of ventilation, occupant density and dwell time (Bazant and Bush, 2021). CFD-based studies have been used to examine ventilation performance, aerosol dispersion and mitigation strategies for COVID-19 transmission in buildings and transport settings broadly (Mohamadi and Fazeli, 2022). For example, a recent study in a train carriage couples Wells–Riley with CFD, demonstrating the value of integrating airflow physics with probabilistic infection calculations (Wang et al., 2022). In addition, a study of Diamond Princess outbreak finds that airborne spread played a major role in the COVID-19 spread using mechanistic transmission modelling (Azimi et al., 2021). By contrast, ABM focus on the spatio-temporal interactions and movement patterns of individuals, providing high-resolution representations of how people traverse, occupy and use space.

The application of ABM tools is particularly relevant in the context of cruise ships, where space is often limited, and passenger flow must be carefully managed to prevent overcrowding and ensure safety and satisfaction. Cruise ships differ fundamentally from many other indoor settings previously studied such as classrooms or transit spaces due to the extended exposure duration, high-density mixed-use spaces, complex behavioural and movement patterns and specialised HVAC systems (Xia et al., 2023). Therefore, ABM can also be utilised to design decks and public spaces that promote efficient use of spaces and improve the way-finding experience of passengers. Health and safety in infectious disease outbreak and timely evacuation of passengers are critical concerns, and ABM can be employed to test the design and layouts and improve the operational procedures. The ability to model different scenarios allows operators to identify potential weaknesses in deck plans and operational interventions to make evidence-based decisions to enhance passengers' health and safety.

3. Methods

3.1. Framework

This study is based on the unique environment of cruise ships, as a response to the development of healthier cruise ship environments through operation and design initiatives. As shown in Fig. 2, this study starts from the literature review to inform the research gap, understanding the broad background of health risks in cruise ships and how ABM can be used to study the interior environment. Three case studies

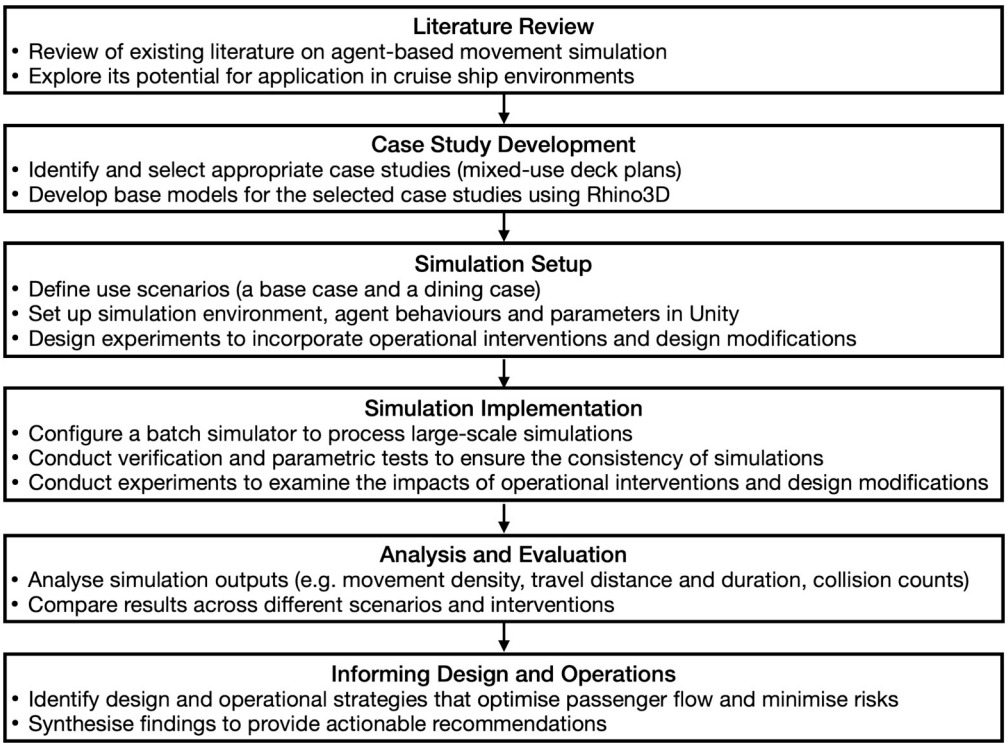

Fig. 2. Research design.

are identified, followed by the development and verification of ABM simulation. Experiments are designed to examine the effects of different design and operation strategies, in order to provide guidance and suggestions.

3.2. Agent-based modelling

This study applies the 'DesignMind' toolkit to develop an agent-based movement simulation model to test different design and operational scenarios in decks of cruise ship case studies. The toolkit (Baur et al., 2023; Gath-Morad et al., 2023) integrates empirical evidence into architectural design and offers insight to inform architects' and designers' decisions. Compared to other types of ABM, this tool has the benefits of being open-source, easy-access and highly adaptive, enabling it to be applied in different scenarios across practice and research.

This agent-based simulation module is built within game engine Unity (Unity Technologies, 2024), taking advantage of its user-friendly 3D visualization capabilities and robust programming backend for coding model logic (Cheliotis, 2021). This section of the paper introduces the key concepts and workflow of the simulation tool, including the environment, the agents and tasks and the key output metrics, as shown in Fig. 3.

3.2.1. Base model and simulation environments

The major input of the agent-based simulation module is 3D building models with basic spatial configurations. This is set as the environment that agents act in (Wurzer et al., 2012). The major origins, destinations and points of interest (POIs) are identified from the 3D model. The details of the models of selected deck plans are discussed in Section 3.3.1. In Unity, one unit of time is assumed to be 1 s, while 1 unit in the

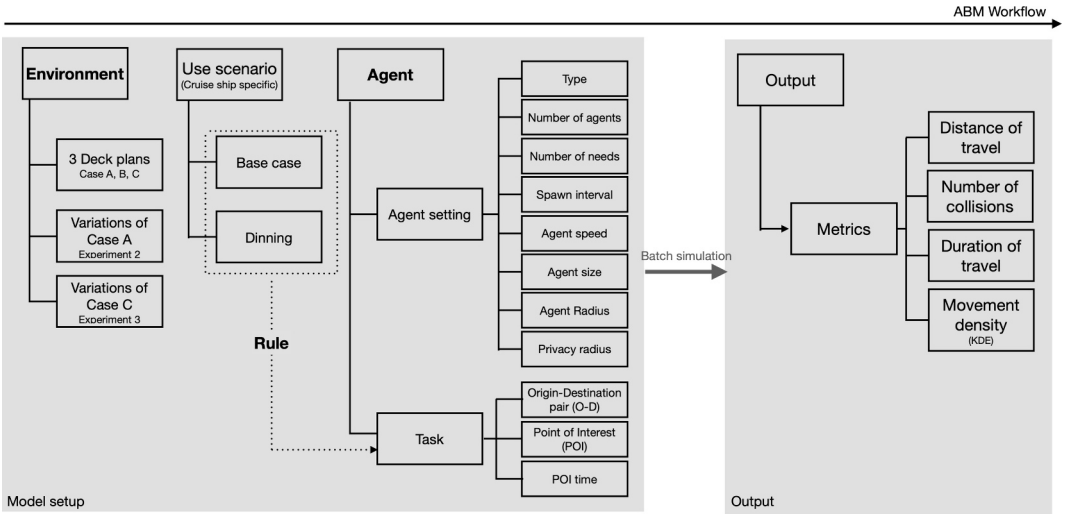

Fig. 3. Workflow of Agent-based simulation.

coordinate system is assumed to be 1 m. A Unity navigation mesh is created from the base model to define the area for pathfinding and movement activities.

3.2.2. Agents and tasks

Agents are defined as the 'active entities within the simulated world' (Wurzer et al., 2012). In movement simulation, the agents represent the occupants in the environment. The simulation can involve different types of agents, each programmed with specific behaviours and tasks.

Agents in the simulation are designed with properties that dictate their behaviour, such as spawn time, number of needs, walking speed, size, radius, time spent at POIs and the privacy radius. Tasks are designed for agents to indicate the starting and ending locations (origins and destinations) and the visits to POIs for the movement. The agents show up and start from the origin, move towards and disappear at the destination, whilst stopping by one or more pre-defined POIs. The agents follow a shortest-path heuristic to navigate between origin, destinations and POIs. A randomisation option is included to reflect the occurrence of various movement patterns in the simulation (Gath-Morad et al., 2023). A batch simulator is configured to accelerate the simulation process.

3.2.3. Dimensions of human mobility

The simulation tool provides several key output metrics that are critical for analysing and interpreting movement behaviour of agents, extracted via a visualiser component. The basic format of output is a table that documents the coordinates of agents at each time point, the number of collisions and the agents' travel distance and duration. The coordinates are further extrapolated to movement density.

Travel distance and duration.

Travel distance and travel duration are two fundamental metrics used to characterise agent movement. Travel distance refers to the cumulative length of the path traversed by each agent throughout the simulation. Travel duration denotes the total elapsed time during which an agent is in motion.

Collision.

Collisions between agents are detected when an agent comes within a pre-defined proximity – 'privacy radius' – of another agent. It represents the close contact between agents and can be used as a proxy to estimate the potential of infectious disease transmission.

Movement density.

Movement density represents the spatial concentration of agent locations over time. It is calculated using Kernel Density Estimation (KDE) from the agents' recorded positions at regular sample intervals (1 unit per frame). KDE is a non-parametric statistical method used to estimate the probability density function of a continuous variable (Silverman, 1998). In this context, it generates a smooth, continuous surface that reflects the relative intensity of movement across space. Along with collisions, density of occupation (or overcrowding) is also known to be related to the risk of disease spread (Shirreff et al., 2024; Zhang, 2024).

To implement KDE, the recorded 2D coordinates of agents are extracted from the output dataset. The bandwidth is automatically determined using Scott's Rule, which adjusts the bandwidth based on the standard deviation of the data and the number of observations. The resulting KDE surface is computed over a 2D grid with a spatial resolution of 1 unit per cell. The distribution of movement density can be visualised in heat maps, to highlight the areas with higher movement density (known as 'hotspots'), thus help identify the spaces that are prone to overcrowding.

3.2.4. Collision as a proxy for close-contact exposure

Collision dynamics of agents could be used to approximate transmission risks from contact processes in pedestrian simulations, to link individual's spatial mobility with the evolution of epidemics (Toroczkai and Guclu, 2007). In this study, infection risk is not modelled with a full transmission probability per se; rather, collision frequency within a set interpersonal radius (1 m) is used as a proxy for close-contact exposure. This choice aligns with both epidemiological evidence and WHO guidance (WHO, 2025): physical distancing of 1 m or more significantly reduces risk of respiratory droplet transmission (Chu et al., 2020). In the health emergency case, the count of collisions between infected agents and normal agents is directly related to the potential for disease transmission (Yamamura et al., 2023). Each collision represents a close contact between agents, where transmission may occur. As the number of collisions increases, the chances of more agents getting infected also rise. Such count of collisions could be further extended to the estimation of infection possibility by combining with the data about transmission rate, however, this is currently out of the scope of this study.

In confined indoor environments like cruise ship corridors and dining spaces, interpersonal proximity typically precedes or coincides with body-contact events, and therefore collision frequency provides a conservative indicator of moments when interpersonal distance is insufficient to prevent pathogen transmission. While this proxy does not explicitly model aerosol or fomite transmission (Christakis and Drikakis, 2024; Sovatzidi et al., 2024), it effectively captures behaviourally grounded, spatially explicit interactions that are likely to generate high-concentration risky moments.

3.3. Case-specific analysis and experimental setups

While the previous section introduces the fundamentals about the ABM tool, this section focuses on the introduction of case-specific analysis, including a description of selected case studies, calculation of spatial characteristics, proposed scenarios and the settings of tests and experiments.

3.3.1. Case studies

Three cases (denoted as Case A, B and C) were selected as the base environments for running the agent-based simulations, following a convenience sampling rule. The selection of cruise ships and deck plans was informed by the 'Healthy Ship for you' (HS4U) project consortium (CORDIS, 2022). Mixed-use decks were chosen because they include both cabin areas and public spaces, providing a diverse environment for analysis across the entire deck to incorporate various scenarios and setups for agent behaviour (Cotfas et al., 2023).

While the detailed plans for Case A were provided by industry partners in the consortium, the other two deck plans (Case B and C) were extracted from publicly available sources (CruiseMapper services, 2024). The 3D models of the selected decks were constructed in Rhino3D (McNeel, 2024). The analysis focuses on the horizontal movement within a single deck, while the vertical circulation and possible transmissions in stairways and elevators are not considered. The information and plans of the cases are shown in Table 1 and Fig. 4. In these plans, the grey areas represent passenger-inaccessible zones, whereas the white areas are all accessible for generating the navigation field in Unity.

Case A.

Case A is in a large cruise vessel and corresponds to Deck 5 with an area of 7045 m^2. This deck accommodates 27 accessible inside cabins and 46 outside cabins (i.e. with windows), along with additional crew rooms. Circulation is supported by 10 elevators, 3 large staircases and 3 smaller staircases. For this study, only a portion of the deck – referred to as the studied area – was included in the simulation. The excluded part includes a large restaurant and bar, which are separated from the studied area by an inaccessible galley. The simulated area (3687 m^2) comprises the embarkation zone, a grand foyer, a smaller restaurant (22 tables, 78 seats), reception areas and the cabins.

Case B.

Case B represents Deck 4 of a medium-sized vessel, with a total area of 3876 m^2. The deck includes cabin areas, public amenities and a dining space, served by two central staircases and four elevators. The cabin section is arranged in a grid-like structure with two long corridors connected by three shorter cross-corridors, providing access to 39 inside cabins and 52 outside cabins. Public areas are divided into three main

Table 1
Basic information of three case studies.

		Case A (studied area)	Case B	Case C
Basic information	**Cruise ship capacity**	10 accessible decks 6 decks with cabins 956 staterooms	9 accessible decks 7 decks with cabins 724 staterooms	9 accessible 6 decks with cabins 467 staterooms
	Case study deck	Deck 5 (studied area: the mixed-used part)	Deck 4	Deck 5
	Number of cabins on the deck	73 cabins	91 cabins	42 cabins
	Circulation area	6 Lifts 2 Large staircases	4 Lifts2 Staircases	4 lifts2 Staircases
	Major facilities	Studied area:1 Small restaurant (78 seats) 1 Grand foyer 1 Reception area (8 seats) 1 Toilet	1 Restaurant (728 seats) 1 Reception area 1 Toilet 1 Shore excursion area 1 Duty free & value shop 2 Shop 1 Library 1 Internet cafe	1 Restaurant (188 seats) 1 Reception area 1 Toilet 1 Shore excursion area 1 Duty free & value shop 1 Photoshop
Area (in m^2)	**Total internal area**	7045.06 (whole deck) 3687.12 (studied area)	3876.05	2475.45
	Cabin	1382.67	1019.57	580.64
	Corridor around cabins	328.14	186.35	110.44
	Public area	1198.87	2675.58	1322.22
	Restaurant	156.30 (studied area)	1302.45	400.66

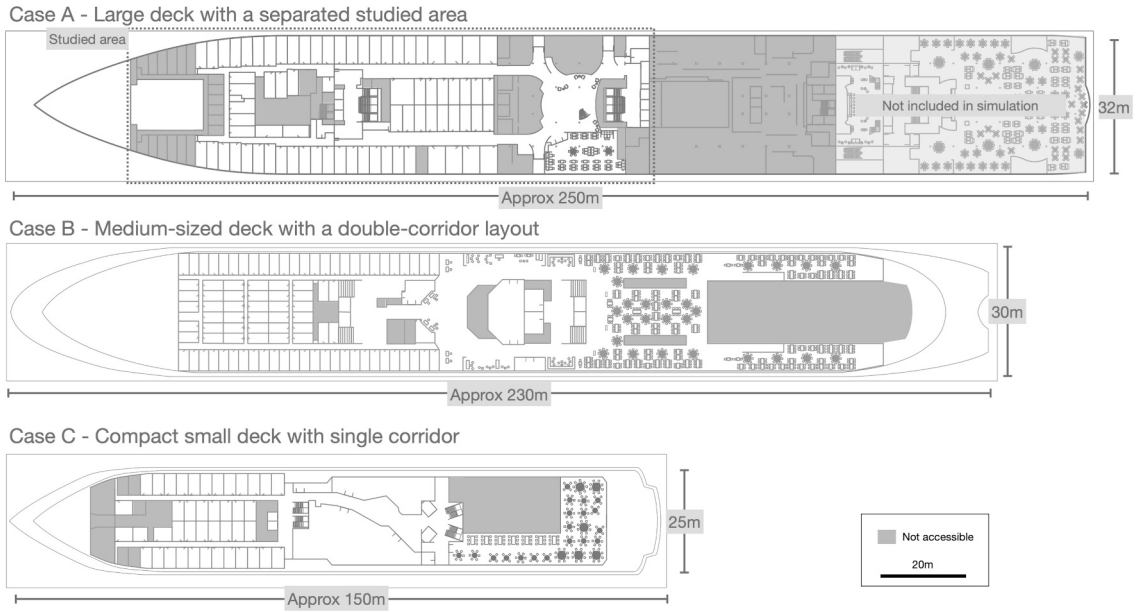

Fig. 4. Deck plans of three cases.

zones by two primary corridors. The central zone includes toilets and a duty-free shop, while side areas include a reception, retail shops, an internet café and a library. A large restaurant with 728 seats is integrated into the public space, with a centrally located galley at the end.

Case C.

Case C is the Deck 5 of a smaller cruise vessel, with a total deck area of 2475 m^2. This deck is characterised by a simpler layout and more concentrated functional elements. The cabin zone consists of two long corridors connecting 18 inside and 24 outside cabins. The public area is organised along a single main corridor that links key facilities, including the reception, duty-free/value shop, photo shop and shore excursions counter. A restaurant with 188 seats is located at one end, adjacent to the galley and storage area. Vertical circulation is provided by four elevators and two large staircases.

3.3.2. Spatial characteristics of case studies

In order to compare the three case studies in terms of their layouts, the spatial characteristics of each deck were assessed using two complementary approaches: (1) basic spatial metrics that describe the physical layout and functional composition of space, and (2) visibility-based analysis using space syntax theory to quantify how spatial design influences perception and movement.

The basic spatial metrics calculate a set of geometric and functional indicators that characterise the distribution, shape and allocation of different space types:

- Occupancy Density represents the average amount of floor area available per individual agent. It is calculated by dividing the total

area of the deck by a standardised simulated population (100 agents).

- Shape Index and Compactness Ratio capture the geometric compactness or irregularity of a spatial layout. They are defined as the ratio of the perimeter to the area of the space (as shown in the following equations Eq. (1) and Eq. (2) (Bardhan et al., 2024, 2018).

$$ShapeIndex = \frac{P}{2\sqrt{\pi A}} \quad (1)$$

$$CompactnessRatio = \frac{4A}{P^2} \quad (2)$$

A Area

PPerimeter

- Corridor-to-cabin ratio: This metric quantifies the relative extent of circulation space (corridors around cabins) in relation to private accommodation (cabins). It is calculated by dividing the total area allocated to corridors around the cabins by the total cabin area.
- Public-to-private ratio: This metric quantifies the balance between communal and individual space. It is calculated as the ratio of public areas to private cabin areas.

Secondly, visibility graph analysis (VGA) was used to quantify the spatial visibility characteristics that influence how people perceive and navigate through space (Turner et al., 2001). VGA is a computational technique derived from space syntax theory which represents space as a network of inter-visible points and quantifies how visual connections vary across a layout. The use of space syntax analysis on vessels has been demonstrated in previous works (Li and Shao, 2021; Moloney, 2018). Four space syntax metrics that were used to describe the spatial design variations:

- Connectivity: The number of directly connected spaces from a given point, representing how easily a space links to others (Hillier and Hanson, 1984).
- Isovist Area: The total visible area from a given point in space with respect to an environment (Benedikt, 1979).
- Through Vision: The extent to which a person can see through multiple connected spaces, measuring spatial transparency (Turner et al., 2001).
- Visual Integration: How visually accessible a space is within the entire layout, with higher values indicating central, well-connected areas. A well-integrated space is shallow to all other locations, while a poorly integrated location is deep (UCL Space Syntax, 2024).

Appendix A presents the full space syntax descriptive data of case studies that were subsequently analysed in relation to ABM results.

3.3.3. Proposed scenarios on deck movements

Two ABM simulation scenarios were developed based on the functional layout and spatial characteristics of selected mixed-use decks, to reflect typical patterns of passenger activity. The two scenarios represent different movement behaviours: a random walk scenario and a directive walk scenario (focused on dining activity which a key risk factor in potential disease spread).

Random walk – Base case.

In the base case scenario, agents are programmed to move around the deck with their start and end points set in cabin rooms and major circulation areas like lifts and staircases. The selection of routes and points of interest (POIs) is fully randomised to simulate natural, unstructured movement patterns. This scenario establishes a baseline for the comparison of key output metrics, such as movement density and collision rate across different scenarios, layouts and interventions. The base case serves as a control scenario for more complex situations.

Directive walk – Dining Scenario.

The dining scenario simulates structured, goal-oriented movements. In this scenario, agents move from their cabins and circulation areas to dining seats, where they remain for a fixed period before returning to cabins or going towards other circulation areas. This scenario models peak-time crowding in food service environments – typically considered high-risk due to the density of people in enclosed spaces with prolonged contact durations. It is critical for understanding how crowding in dining areas can be managed.

Table 2
Summary of all simulations.

	Scenario	Agent setting	Deck plan	Number of simulation runs (n)
Verification Test (VT)	**Base case**	**Default**	**Case A, B, C**	n = 50 for each case
	Dinning	**POI time changed to 10**	**Case A, B, C**	n = 50 for each case
Parametric Test (PT)	**Base case**	**Change in number of agents**	**Case A, B, C**	n = 101 for each case
	Base case	**Change in spawn interval**	**Case A, B, C**	n = 5 for each case
	Base case	**Change in number of needs**	**Case A, B, C**	n = 5 for each case
	Base case	**Change in agent size**	**Case A, B, C**	n = 5 for each case
	Base case	**Change in agent radius**	**Case A, B, C**	n = 10 for each case
	Base case	**Change in privacy radius**	**Case A, B, C**	n = 16 for each case
	Base case	**Change in POI time**	**Case A, B, C**	n = 5 for each case
Experiment 1	**Base case**	**Two types of agents (Infected agents and normal agents) are used. Details introduced in Section 3.5.3.3.**	**Case A, B, C**	n = 360
Experiment 2	**Base case**	**Default**	**Case A, original plan (EXP2)**	n = 10
	Base case	**Default**	**Case A, variation 1 (EXP2a)**	n = 10
	Base case	**Default**	**Case A, variation 2 (EXP2b)**	n = 10
	Base case	**Default**	**Case A, variation 3 (EXP3b)**	n = 10
Experiment 3	**Base case**	**Default**	**Case C, original plan (EXP3)**	n = 10
	Base case	**Default**	**Case C, variation 1 (EXP2a)**	n = 10
	Base case	**Default**	**Case C, variation 2 (EXP2b)**	n = 10
	Base case	**Default**	**Case C, variation 3 (EXP3b)**	n = 10
Total number of simulations:				**1181**

Table 3
Default agent setting in the simulation.

Setting	Default parameter	Explanation of the setting (adapted from Baur et al., 2023)
Number of agents	100	The total number of agents involved in the simulation task.
Spawn interval	1	The time interval (in simulation units) between the spawning of successive agents.
Agent type	Passenger	The predefined behavioural profile assigned to each agent
Number of needs	1	The number of POI needs that each agent will fulfil before terminating its movement sequence.
Agent speed	1	The agent's movement speed, expressed in simulation units per time step.
Agent size	0.8	The physical size of each agent used for scaling within the simulation environment.
Agent radius	0.5	The minimum distance maintained from the agent's centre to prevent overlap with others – used for collision avoidance and spatial negotiation.
Privacy radius	1	The proximity threshold around an agent used to detect and record collisions.
POI Time	1 (base case) 10 (dinning case)	The amount of time an agent remains at a point of interest.
Revisit	TRUE	Indicates whether agents are allowed to revisit previously visited POIs. If set to true, revisitation is allowed during the simulation.
Choose non-deterministically	TRUE	Specifies whether the selection of the next POI is made randomly from the remaining available options. If true, agents choose non-deterministically.

3.3.4. Tests and experiments

This section outlines the simulation settings, with two major components: (1) verification and parametric tests and (2) experimental scenarios. This structure follows a previous ABM study on movements in offices (Yu, 2023), and is adapted to the context of cruise ship design. Table 2 summarises all simulation runs conducted across the tests and three experiments. A total of 1181 simulations was performed. In this study, n refers to the number of simulation runs, and n_{agent} denotes the number of agents involved.

The number of simulation runs was determined based on methodological practices in prior agent-based modelling research (Yu, 2023, 2022), computational feasibility and the variance characteristics of the model. Previous studies typically conducted 10 runs for verification purposes to assess model stability and relied on a single run for experimental condition. The model in this study has a relatively small agent population (maximum of 100 agents) and demonstrates limited variance, while the use of the Unity game engine requires approximately 4–5 min per simulation. As a result, simulation runs were configured as follows: (1) Verification tests were repeated 50 times per case and per scenario to examine output consistency under controlled conditions; (2) Parametric tests have one run per setting; and (3) Experiments were repeated 10 times for each.

Table 3 presents the default parameter settings. The agent population ($n_{agent} = 100$) was estimated based on the number of staterooms in each deck layout and held constant across the three deck plans. This standardisation facilitates comparisons of outputs across different spatial configurations. A population of 100 agents represents a sufficiently large yet computationally tractable sample for observing emergent patterns in movement behaviour and hotspots.

A spawn interval of 1 time unit was adopted to enable a continuous but evenly distributed flow of agents into the environment. Other parameters were derived from standard human-centred design references (Neufert et al., 2012). For example, agent speed is set uniformly at 1 unit per time step, approximating typical indoor walking speed. Agent size is set to 0.8 to reflect a scaled representation of the Unity Humanoid capsule, while the agent radius is set to 0.5 to define the personal space around each agent, creating a buffer zone for collision avoidance. The privacy radius of 1 unit represents a slightly extended personal space threshold used to detect close contacts between agents, consistent with social distancing guidance (e.g. 1 m separation).

Table 4
Setting variations in parametric tests.

Parametric Test (PT)	Parameter	Test range	Increment per run
Parametric Test 1 (PT1)	Number of agents	1 to 100 agents	+1 agent
Parametric Test 2 (PT2)	Spawn interval	1 to 5 units	+1 unit
Parametric Test 3 (PT3)	Number of needs	1 to 5 needs per agent	+1 need
Parametric Test 4 (PT4)	Agent size	0.6 to 1.0 units	+0.1 unit
Parametric Test 5 (PT5)	Agent radius	0.1 to 1.0 units	+0.1 unit
Parametric Test 6 (PT6)	Privacy radius	0.5 to 2.0 units	+0.1 unit
Parametric Test 7 (PT7)	POI Time	1 to 5 units	+1 unit

3.3.4.1. Verification test. A verification test is a fundamental step to assess the internal consistency, stability and reliability of simulation outputs under repeated, controlled conditions. In this study, verification tests were conducted to ensure that the simulation model behaves as expected when the same input parameters are applied in multiple runs before proceeding to experiments.

For each scenario across the three case studies, 50 simulation runs were conducted using the default parameter settings. The verification tests serve multiple purposes: they establish the validity of the simulation outputs, allow observation of the output distributions and enable exploration of relationships between key output metrics. Furthermore, they provide insight into baseline movement patterns, facilitating comparison between the three case studies and across the two behavioural scenarios (random walk and directive walk). Analysis focuses on aggregated simulation-level outputs, such as average travel distance, number of collisions and travel duration in each simulation run, as well as agent-level data.

3.3.4.2. Parametric test. Parametric test was conducted to examine the sensitivity of model outputs to changes in key simulation parameters with 'one-factor-at-a-time' method (Smajgl and Barreteau, 2014a). This stage helps identify which variables exert the most significant influence on outcomes, thereby supporting the interpretation of results.

In each parametric test, a single parameter was systematically varied within a plausible range while all other variables were held constant at their default values (see Table 4). Seven parametric tests (PT) were performed with the base case scenario, each corresponding to a specific variable: number of agents (PT1), spawn interval (PT2), number of needs (PT3), agent size (PT4), agent radius (PT5), privacy radius (PT6) and POI time (PT7).

For each setting, a single simulation run was conducted due to computational feasibility. The variation of each parameter is analysed in relation to three key output metrics: mean travel distance, mean number of collisions and mean travel duration.

3.3.4.3. Experiments. Three simulation experiments were conducted using the base case model. These experiments were designed to explore

movement behaviour under variable conditions: risk level of infection spread, operational intervention for restricted access and variations in spatial layout.

To assess the magnitude of differences between original case (Case A and C) and alternatives in Experiments 2 and 3, the effect sizes are calculated using Hedge's *g*. Hedge's *g* standardises the mean difference by the pooled standard deviation and corrects for small sample bias, which is particularly appropriate for comparisons with unequal or small sample sizes (smaller than 50).

Hedge's *g* is calculated using Eq. (3), while the bias correction term is expressed as Eq. (4):

$$g = \frac{\overline{y_1} - \overline{y_2}}{s_p} \tag{3}$$

where: $\overline{y_1}, \overline{y_2}$ are sample means

s_p is the pooled standard deviations, computed as:

$s_p = \sqrt{\frac{(n_1-1){s_1}^2+(n_2-1){s_2}^2}{(n_1-1)+(n_2-1)}}$, s_1 and s_2 are the sample standard deviations.

The bias correction term is

$$\frac{n-3}{n-2.25}\sqrt{\frac{n-2}{n}} \tag{4}$$

n is the total sample size $n_1 + n_2$.

Experiment 1: Potential of infection spread.

The first experiment aims to explore the potential for infection transmission as a function of the infection prevalence and overall population density. Collisions within privacy radius are used as a proxy for potential transmission events.

Two agent types are defined: infected agents and non-infected (normal) agents. Infected agents are assigned a privacy radius of 2 units to record proximity-based collisions with normal agents, in line with standard social distancing requirements (e.g. during the COVID pandemic). Normal agents retain the default setting with a privacy radius of 1 unit. The more agents that collide with infected agents, the higher the possibility that normal agents may get infected. The simulation varies both the population size (50 and 100 agents) and the proportion of infected agents (ranging from 1 % to 20 %), as listed in Table 5. A total of 360 simulation runs were conducted under different combinations of agent numbers and infection ratios.

Experiment 2: Access restriction to cabin zones for quarantine or treatment purpose.

This experiment investigates the impact of operational-level quarantine interventions on agent movement. It simulates restricted access to designated corridor segments and cabins, reflecting a real-world quarantine setup scenario in which parts of the cabin area are sealed off, for the purpose of creating a temporary quarantine or hospital/treatment zone in health emergencies.

The modifications were applied to Case A, producing three variations (Cases A1, A2, and A3), each implementing access restriction zones at different positions along the corridor, illustrated in Fig. 5:

- Case A1 – Restricted access at the front of the corridor
- Case A2 – Restricted access in the middle of the corridor
- Case A3 – Restricted access at the end of the corridor

In each case, 15 cabins were designated as quarantined, with access fully blocked. This setup allows for analysis of how the spatial position of restricted areas affects movement efficiency, overcrowding and behavioural rerouting.

Experiment 3: Design Modifications.

The third experiment evaluates how spatial layout modifications influence movement patterns. It tests the performance of three alternative corridor and cabin arrangements based on the original layout in Case C.

The modifications preserve the number of outward-facing cabins while reconfiguring only the internal cabin blocks. While the original layout only has two parallel corridors, the three design variations are:

- Case C1 – 'Racetrack': A new corridor is added at the back, connecting the two parallel corridors.
- Case C2 – 'Perpendicular grid': A central corridor intersects the parallel corridors in the middle of cabin area.
- Case C3 – 'Tapering grid': The central corridor is widened by rotating inner cabins from portrait to landscape orientation.

The total number of cabins varies slightly among the layouts: 42 cabins in Case C1, 40 in Case C2 and 39 in Case C3. The layouts are detailed in Fig. 6.

4. Results: Verification and parametric test

4.1. Verification test

4.1.1. Verifying the simulation results

The verification tests confirm that the modelling tool exhibits a reasonable degree of internal consistency. Fig. 7 illustrates the average output values from each simulation run across three cases under two scenarios, while detailed descriptive statistics are provided in Appendix B.

Among the three output metrics, average distance shows the least variability, with narrow interquartile ranges and low standard deviations. In contrast, both average number of collisions and average duration show greater fluctuation across simulation runs, as indicated by the presence of outliers, wider output ranges and higher standard deviations.

To further assess output stability, two comparative measures were used: (1) the range-to-mean ratio and (2) the coefficient of variation.

Table 5
Setting variations in Experiment 1.

Experiment 1	Case	Infected agent proportions (%)	Number of Infected agents	Number of normal agents
Total number of agents = 50	Case A, B, C	2 %	1	49
Total number of agents = 50	Case A, B, C	4 %	2	48
Total number of agents = 50	Case A, B, C	8 %	4	46
Total number of agents = 50	Case A, B, C	10 %	5	45
Total number of agents = 50	Case A, B, C	20 %	10	40
Total number of agents = 100	Case A, B, C	1 %	1	99
Total number of agents = 100	Case A, B, C	2 %	2	98
Total number of agents = 100	Case A, B, C	4 %	4	96
Total number of agents = 100	Case A, B, C	5 %	5	95
Total number of agents = 100	Case A, B, C	8 %	8	92
Total number of agents = 100	Case A, B, C	10 %	10	90
Total number of agents = 100	Case A, B, C	20 %	20	80
	Note: Privacy radius of infected agents is 2; privacy radius of normal agents is 1			

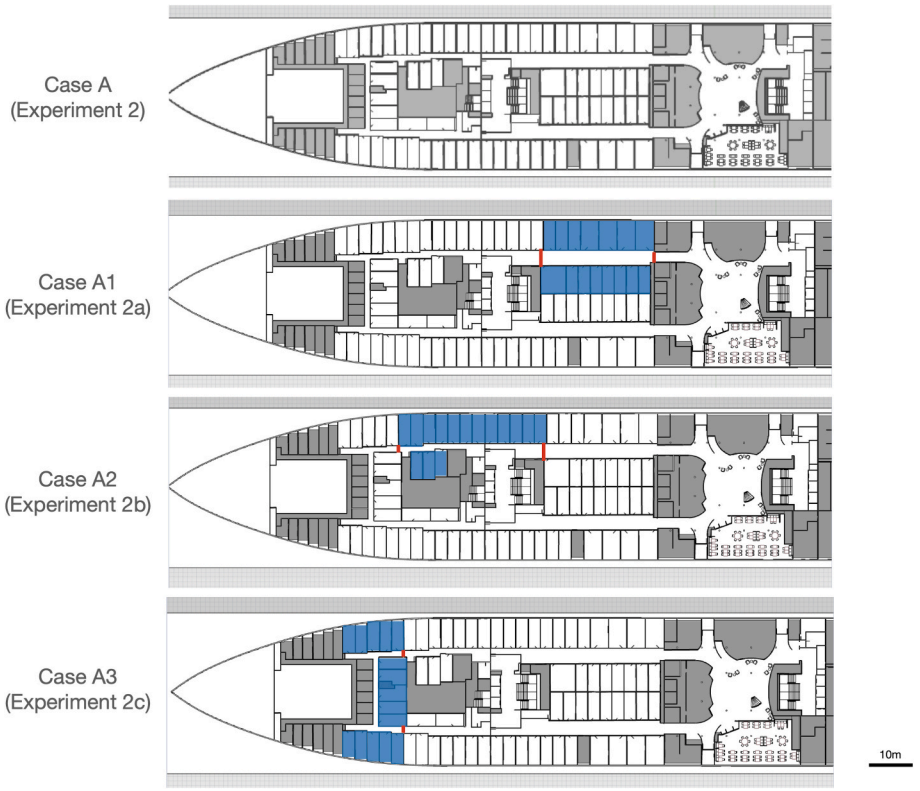

Fig. 5. Deck plans of Experiment 2.

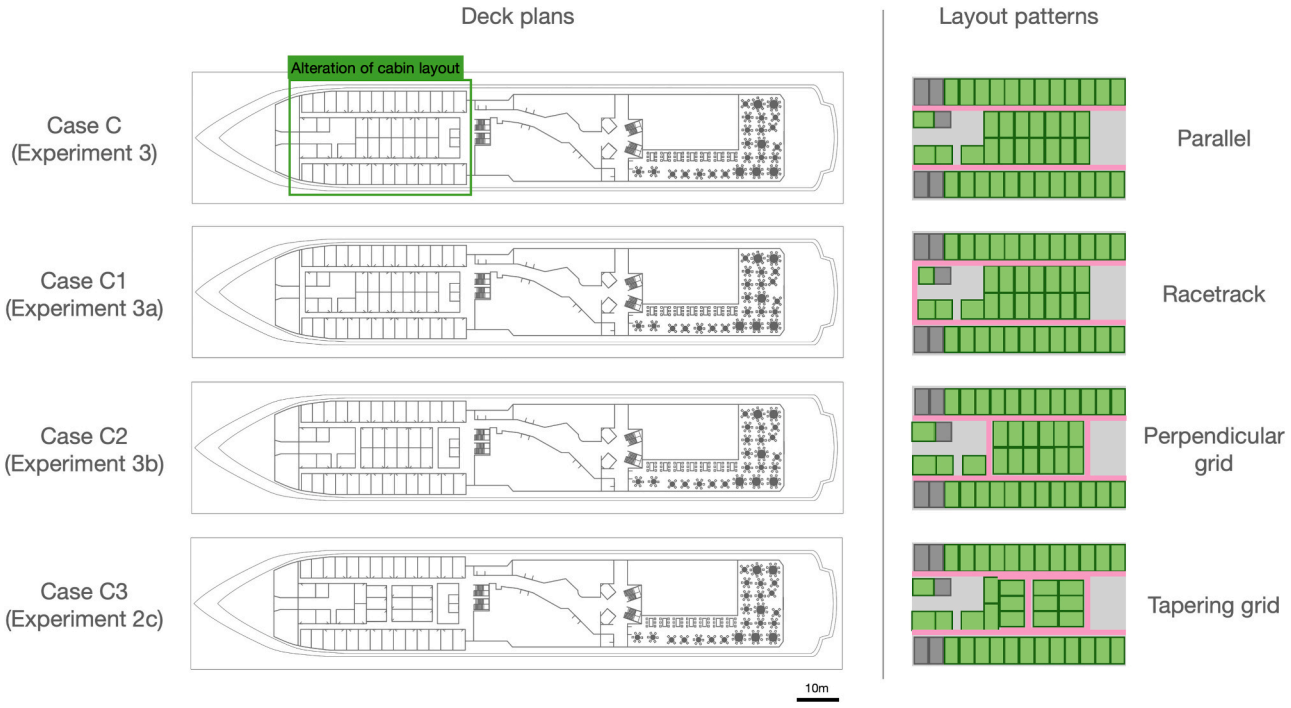

Fig. 6. Deck plans of Experiment 3.

Across all output metrics, the range-to-mean ratio, as a relative measure of data spread, falls between 8.55 % and 48.28 %. The coefficient variation, which reflects variability relative to the mean, ranges from 2.17 % to 12.78 %. These measures consistently confirm that the average distance is the most stable and reliable output, with relatively low sensitivity to stochastic variation. In contrast, the number of collisions and duration are more volatile, particularly in Case C, which shows the highest relative variation among all cases. The observed variability remains within an acceptable range when compared to findings reported in previous studies (Yu, 2023).

Fig. 8 shows the distribution of individual-level agent outputs, based on 5,000 agents per case-scenario combination. A Shapiro-Wilk test was

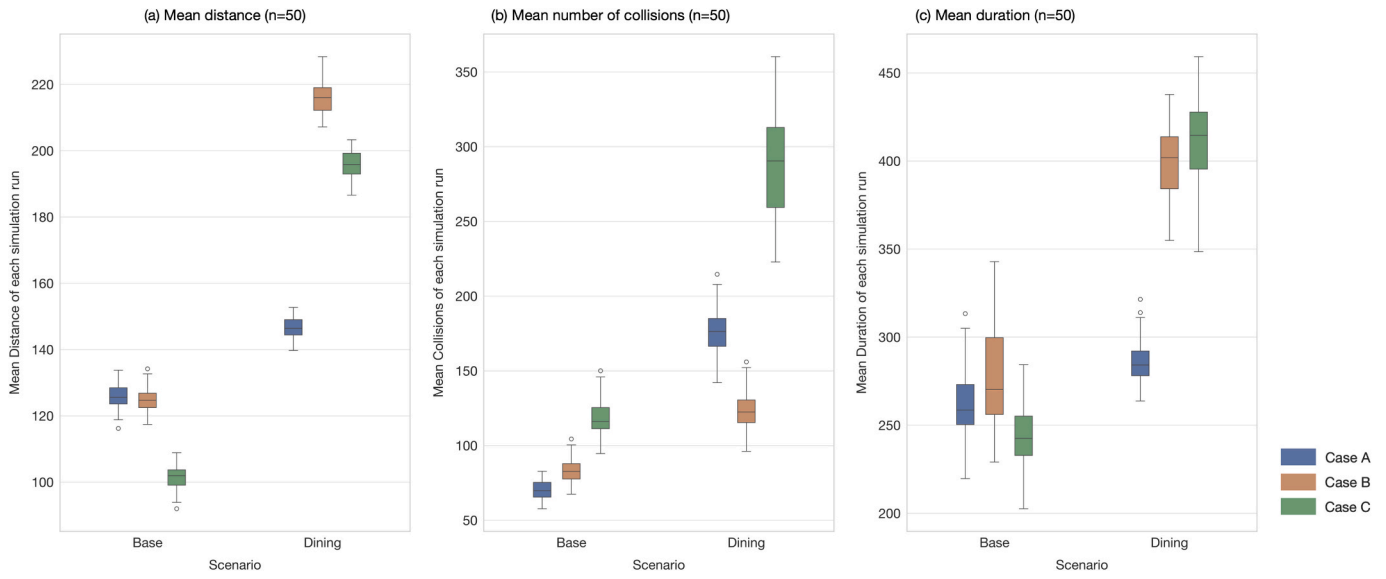

Fig. 7. Results of verification test in box plot, the average values of each simulation (n = 50): (a) Mean distance; (b) Mean number of collisions; (c) Mean duration.

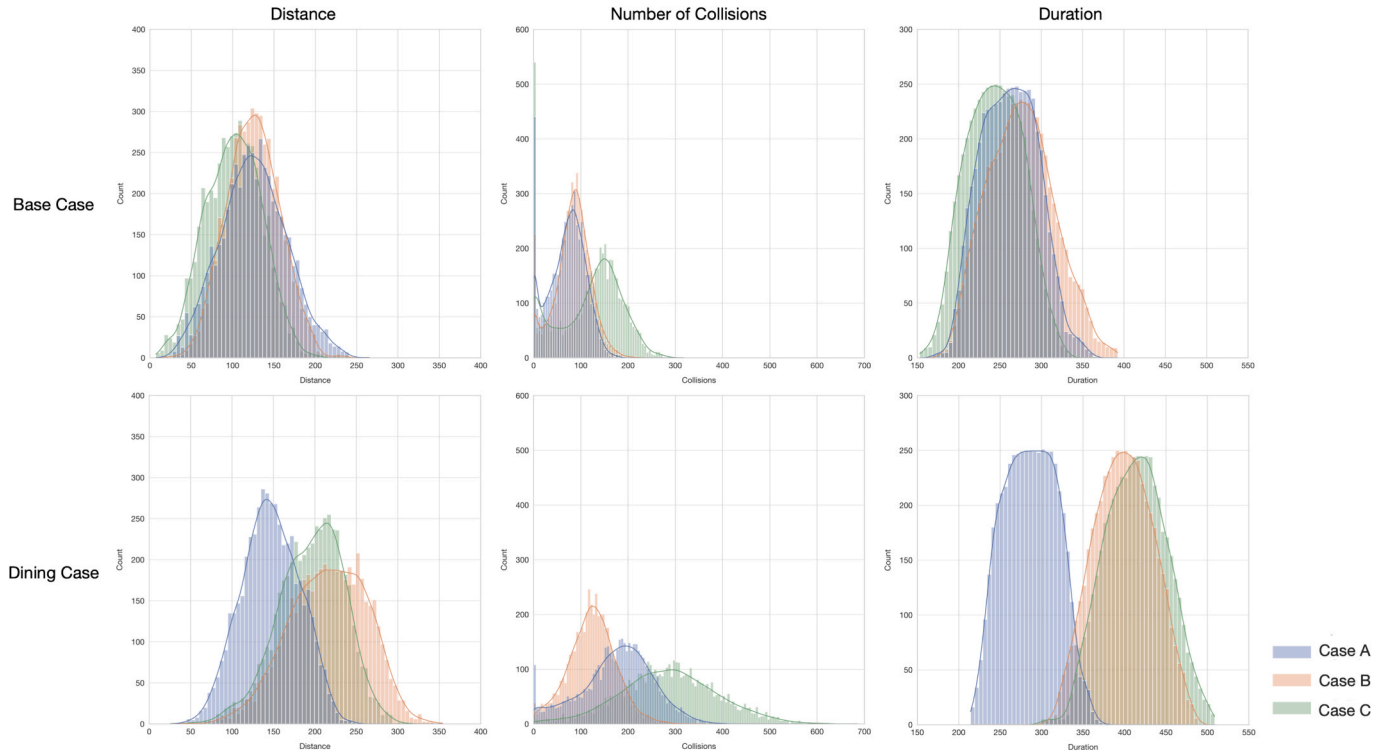

Fig. 8. Results of verification test in histogram, the distribution of distance, number of collisions and duration for each agent, in two different scenarios (n_{agent} = 5000 in 50 simulation runs in each diagram).

conducted to assess the normality of the distributions for all three metrics across 18 combinations. However, all p-values are very significant ($p < 0.05$) across all cases, indicating that none of the output distributions follow a normal distribution. This observation is different from previous study which assumes the outputs follow a Gaussian distribution for further comparison (e.g. Yu, 2023).

To investigate potential interdependencies between the output metrics, Fig. 9 explores three pairwise relationships: distance vs. number of collisions, duration vs. number of collisions and duration vs. distance. Pearson correlation coefficients indicate statistically significant positive correlations in all three cases ($p < 0.05$). The strongest correlation is observed between duration and distance ($r = 0.63$), followed by duration and collisions ($r = 0.59$). The relationship between distance and collisions is notably weaker ($r = 0.30$). Linear trend lines plotted by case further reveal that Case C consistently exhibits steeper slopes across all three pairs, suggesting a heightened sensitivity of its output dynamics.

4.1.2. Observations of the movement pattern

After demonstrating the consistency and robustness of the model, the verification test results also allow for analysis of emergent movement patterns under different scenarios in different cases.

A comparison between the base and dining scenarios reveals that the

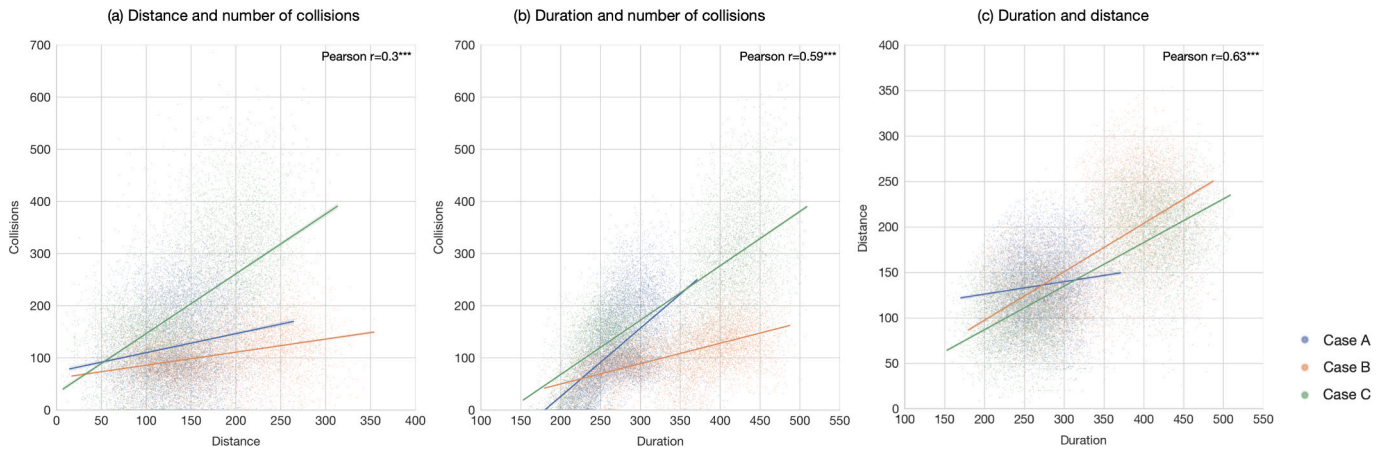

Fig. 9. Pair-wise relationships of three output metrics in verification test (n_{agent} = 30000 in 300 simulation runs in each diagram).

Table 6
Spatial characteristics of the three decks.

		Case A (studied area)	Case B	Case C
Calculated metrics	**Occupancy density (Number of agents = 100)**	70.45 m^2 per agent (whole deck) 36.87 m^2 per agent (studied area)	38.76 m^2 per agent	24.75 m^2 per agent
	Shape Index	1.67 (whole deck) 1.37 (studied area)	1.63	1.60
	Compactness ratio	0.11 (whole deck) 0.17 (studied area)	0.12	0.12
	Ratio: Corridor-to-cabin	0.24	0.18	0.19
	Ratio: Public-to-private (cabins)	0.87	2.62	2.28
Space syntax metrics (Average)	**Connectivity**	57.38	217.99	127.61
	Isovist area	72.77	216.77	132.26
	Through vision	437.20	3874.43	1153.83
	Visual integration	19.57	7.04	179.57

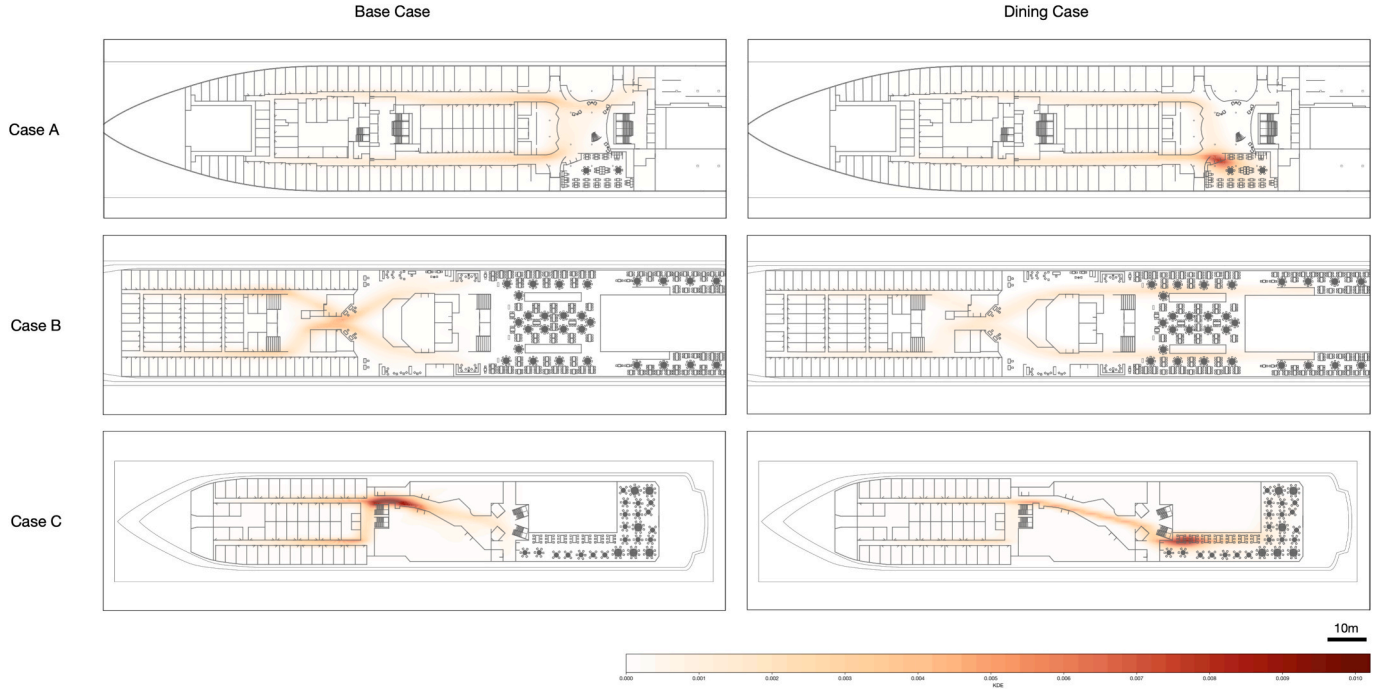

Fig. 10. Results of verification test: Kernel Density Estimation heat map (n = 50 in each diagram).

introduction of dining activities significantly alters movement dynamics. As shown in Fig. 7 and 10, the dining scenario has increased travel distances, durations and collisions, also produces greater variability in number of collisions. This is likely due to agents needing to travel longer to access dining areas, which modifies their random walk patterns, leading to localised congestion and longer time spent at dining seats. The increased collisions from congestions and overcrowding are particularly apparent for Case C.

Table 6 summarises the spatial characteristics of the three case studies. The studied area in Case A demonstrates a mid-range occupancy density and a higher corridor proportion, but a lower public-to-private space ratio. Case B features greater openness and connectivity, with a large public-to-private space ratio and longer visual and movement lines. In contrast, Case C has a dense and compact layout, with the lowest amount of space per agent and more concentrated visibility.

Each case study presents distinctive features that shape movement pattern. Case A supports efficient circulation within a more private and navigable environment. It records the fewest collisions in the base case and exhibits shorter and more stable movement durations and distances, particularly in the dining scenario. Case B exhibits the most expansive spatial structure, with greater visual openness and stronger connectivity. The longer movement paths directly result in higher travel distances and durations, especially when agents move toward the dining area. The large dining area effectively reduces the number of collisions during dining. Case C, as the most compact deck layout, is densely populated and shows the lowest travel distance and duration in the base case. It has very high collisions in both scenarios, possibly due to limited corridor area and high visual integration, which may concentrate movement into narrow pathways. The high mean duration and collisions in the dining case also indicates navigational complexity. Collision data show high variability, possibly reflecting congestion and overcrowding in some simulations – indicative of spatial pressure.

From the KDE maps (Fig. 10), corridors consistently emerge as highly concentrated areas of movement, aligning with findings in other contexts such as office environments (Pan et al., 2021). Corridor widths around cabin areas in each deck plan vary slightly: in Case A, the widest section reaches approximately 3 m, while the narrowest is about 1.3 m. In Case B, corridor widths range from 0.8 m to 1.5 m, whereas in Case C, corridors are slightly narrower, averaging around 1.25 m. Bottlenecks typically occur at junctions where corridors intersect or merge, particularly where agents transition from cabin to public areas.

Additional congestion is observed at restaurant entrances, especially in Cases A and C. In contrast, Case B – featuring the largest dining area – records the lowest collision rates during dining. This may be attributed to its open-plan layout, where no specific restaurant entrance is defined, thereby avoiding bottlenecks.

Overall, the spatial logic embedded in each case – ranging from corridor provision and density to visibility and public/private ratios – helps explain the emergent movement patterns captured in the simulations.

Table 7
Regression relationship in PT1.

		Slope	Intercept	R-squared	p-value
Mean distance	**Case A**	0.04	123.28	0.12	0.00 (significant)
	Case B	0.16	109.40	0.60	0.00 (significant)
	Case C	0.13	88.66	0.49	0.00 (significant)
Mean number of collisions	**Case A**	0.50	24.02	0.80	0.00 (significant)
	Case B	1.22	–32.40	0.81	0.00 (significant)
	Case C	1.18	6.59	0.75	0.00 (significant)
Mean duration	**Case A**	0.78	187.90	0.50	0.00 (significant)
	Case B	1.18	182.64	0.49	0.00 (significant)
	Case C	0.92	146.28	0.72	0.00 (significant)

4.2. Parametric test

The parametric tests were conducted to understand the sensitivity of model outputs to changes in input parameters. The parametric tests validate that these outputs align with expected behavioural patterns in most cases.

Fig. 11 presents the results of PT1, in which linear regression was used to estimate the relationship between the number of agents and the mean values of three output metrics. Descriptive statistics for the regression models are provided in Table 7. A clear linear relationship is observed, particularly between the number of agents and the number of collisions, with relatively large slopes and high R-squared values (ranging from 0.75 to 0.81). This indicates that an increase in agent population directly leads to more frequent collisions, as expected. At the same time, the relationships between the number of agents and the other two output metrics – mean travel distance and duration – are relatively moderate, with lower explanatory power, as reflected in the reduced R-

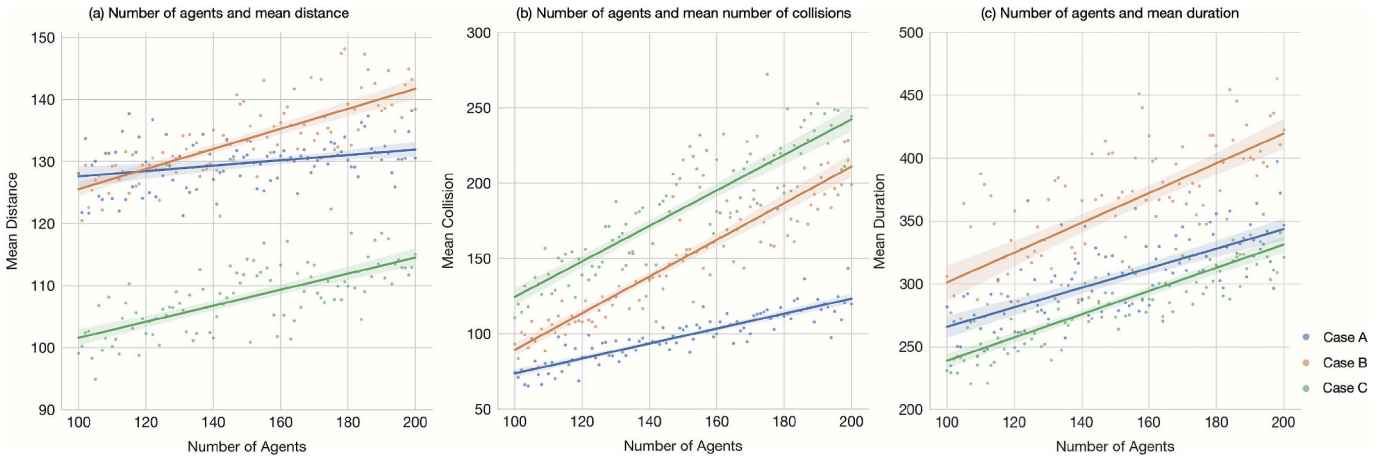

Fig. 11. Parametric test 1, the relationship between the number of agents and the average values of each simulation: (a) Number of agents and mean distance; (b) Number of agents and mean number of collisions; (c) Number of agents and mean duration.

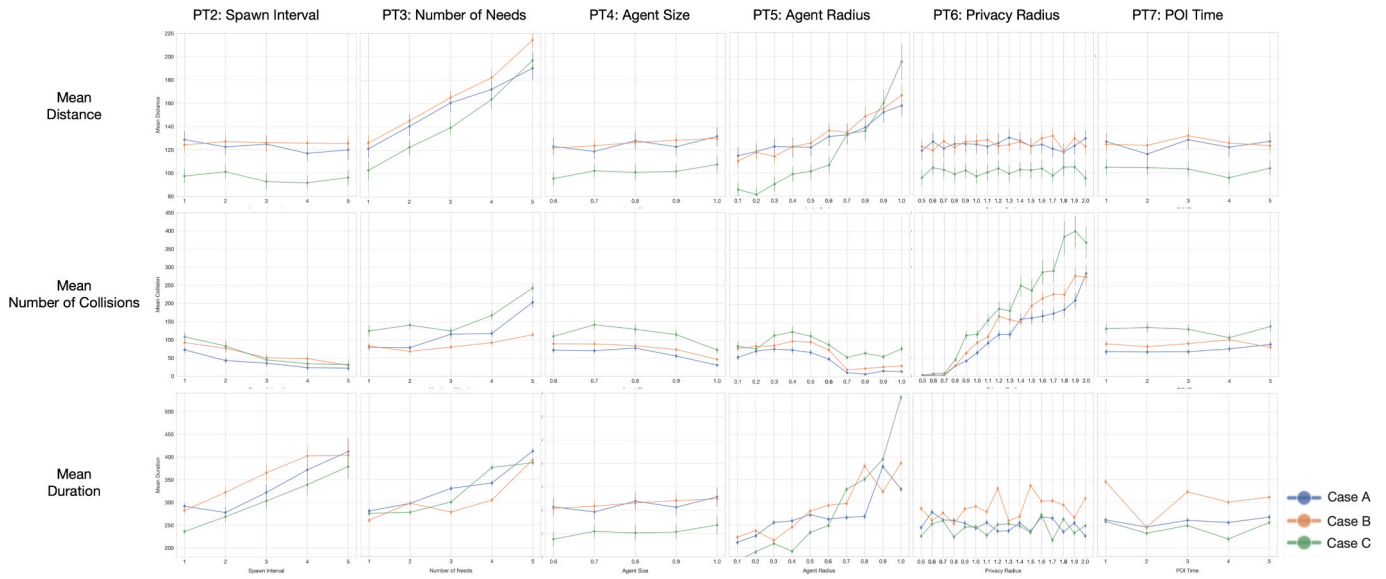

Fig. 12. Parametric test 2 to 7, the relationship between parameters and the average values of each simulation.

squared values.

Fig. 12 illustrates the outcomes of PT2 to PT7, showing the relationships between various parameter values and the average output metrics across all three case studies, under the base scenario. Error bars represent 95 % confidence intervals to enhance the robustness of interpretation, given that each simulation was only repeated once.

Several observations can be drawn from Fig. 12. An increase in the spawn interval reduces the number of collisions but increases the average travel duration, reflecting reduced overcrowding when agents are generated at longer intervals. A higher number of needs consistently leads to increases in all three output metrics, as agents must fulfil more tasks and visit additional POIs. Increasing the agent radius significantly raises travel duration and distance, which is likely due to agents maintaining larger personal buffers to avoid one another, while reducing the likelihood of direct contact. The number of collisions shows a direct correlation with the privacy radius, as it is the primary attribute used to detect collisions, while its effect on the other two metrics remains limited. The influence of agent size and POI time on output metrics appears limited across the tested range of values. Appendix C shows the descriptive results of all PTs for further details.

As a summary, the results from the parametric tests confirm that the model behaves in accordance with theoretical expectations, demonstrating internal validity and reinforcing confidence in the reliability of the simulation framework.

5. Results: Experiments

5.1. Experiment 1: Potential of infection spread

The results of Experiment 1 demonstrate how varying levels of infected agents impact collision rates. The linear regression plots in Fig. 13 reveal strong linear relationships between the number of infected

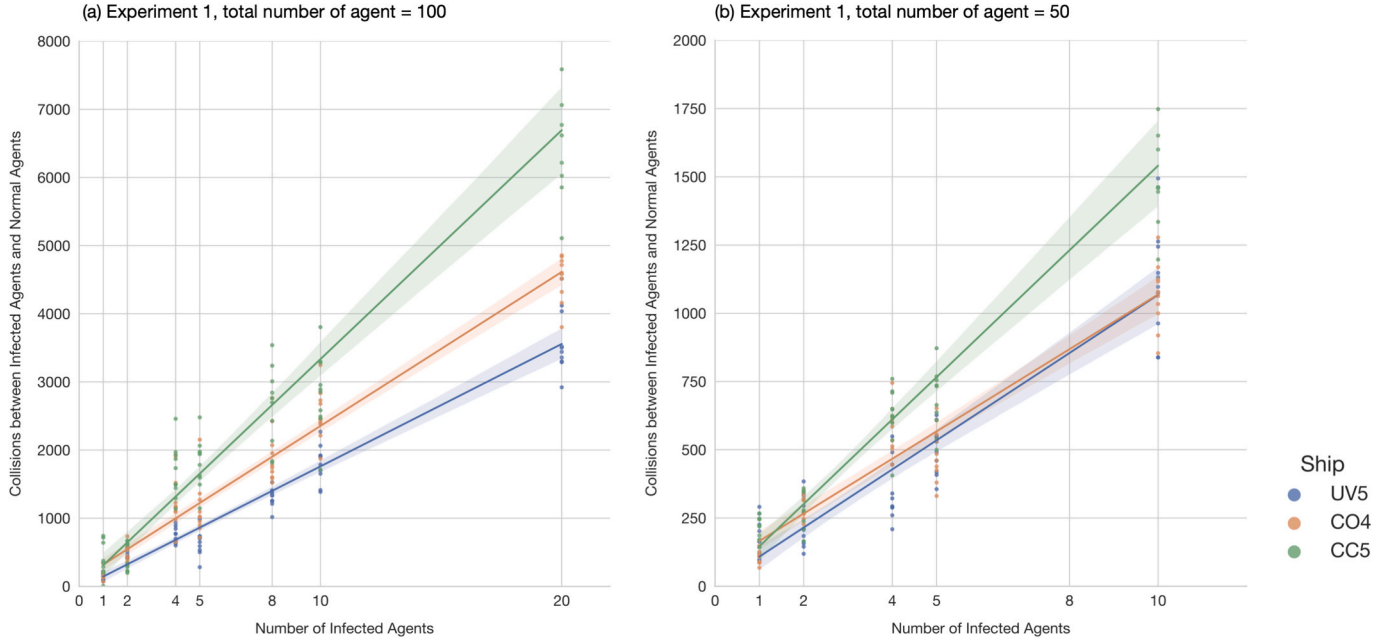

Fig. 13. Results of Experiment 1, relationship between number of infected agents and collisions between infected agents and normal agents: (a) when total number of agents in each simulation is 100; (b) when total number of agents in each simulation is 50.

Table 8
Regression relationship in Experiment 1.

		Slope	Intercept	R-squared	p-value
Total agent number = 100	**Case A**	179.65	−35.59	0.950	0.00 (significant)
	Case B	226.03	93.74	0.945	0.00 (significant)
	Case C	336.01	−25.63	0.912	0.00 (significant)
Total agent number = 50	**Case A**	106.57	2.02	0.876	0.00 (significant)
	Case B	100.37	65.60	0.899	0.00 (significant)
	Case C	154.93	−8.47	0.894	0.00 (significant)

agents and the number of collisions with normal agents, with very high R-squared values. All the R-squared values are over 0.87, as reported in Table 8, indicating that increases in collision rates are largely attributable to higher proportions of infected agents.

Moreover, when the total agent population is doubled from 50 to 100, the number of collisions increases at a disproportionately higher rate. For instance, at 20 % infection, the number of collisions in the 100-agent scenario is more than four times that of the 50-agent scenario. This suggests that in denser environments, the collisions – and by extension, the potential for disease transmission – escalates significantly. When the population of agents is halved by quarantine measures, the reduction in infection risk is dramatically reduced to a quarter.

5.2. *Experiment 2: Access restriction to cabin zones for quarantine or treatment purpose*

This experiment evaluates the impact of operational quarantine measures – implemented as restricted access at different parts along the corridor – on movement patterns in Case A. The baseline (Case A, here referred to as Experiment 2) is compared with three modified configurations: Case A1 (Experiment 2a), Case A2 (2b), and Case A3 (2c), where access is restricted at the front, middle and end of the corridor respectively.

Fig. 14 presents the output metrics as box plots, and Fig. 15 shows the spatial patterns of agent movement using KDE heat maps. Descriptive statistics are included in Appendix D.

Case A1 (Experiment 2a), with restricted access at the front of the corridor, results in the highest average distance, duration and number of collisions. This indicates that this restriction forces agents to take longer detours, leading to concentrated traffic on the other corridor. The result is increased congestion and a significantly higher risk of infection spread via collisions. Case A2 (2b) shows moderate increases in collisions and duration compared to the baseline, while average distance remains close to the baseline. This suggests that mid-corridor restriction leads to partial rerouting, creating localised congestion without substantially elongating routes. Notably, travel duration in A2 is highly variable with a large range, indicating that agents may face varied routing strategies and uneven congestion. Case A3 (2c) reaches the most efficient outcomes, with a notable reduction in travel distance, duration and number of collisions. This configuration appears to minimise unnecessary rerouting, reducing crowding without disrupting general circulation. KDE map also shows more even distribution of traffic, avoiding hotspots. The measurements (Hedge's *g*) of effect size are shown in Table 9.

The location of restriction zones has a substantial effect on both movement efficiency and potential transmission risks. Poorly arranged restrictions – particularly those placed near primary access points – can exacerbate congestion and increase exposure time. In contrast, endpoint restrictions demonstrate potential as a low-disruption strategy that reduces both movement time and interpersonal contact, thereby minimising risk of infection spread. These findings validate the importance of spatially sensitive quarantine and on-board hospital planning in confined environments.

5.3. *Experiment 3: Design alterations*

This experiment investigates how three cabin layout variants (C1 – Perpendicular grid, C2 – Tapered grid and C3 – Racetrack) affect movement patterns compared to the original plan (Case C). As the changes involve only modest adjustments to the internal cabin arrangements, the overall spatial features and ABM outputs exhibit relatively small variations across the four cases. Experiments 3a, 3b and 3c correspond to Cases C1, C2 and C3 respectively, with Case C (Experiment 3 baseline) serving as the reference for comparison. The results are summarised in Fig. 16 (box plots) and Fig. 17 (KDE heatmaps).

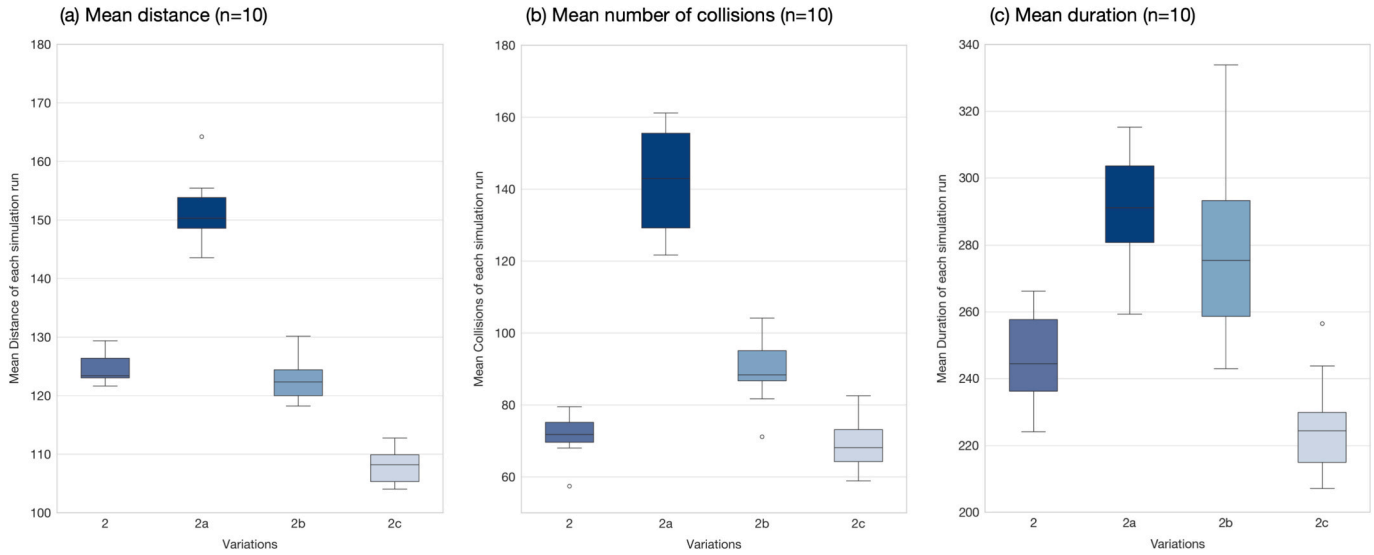

Fig. 14. Results of Experiment 2 in box plot, the average values of each simulation (n = 10): (a) Mean distance; (b) Mean number of collisions; (c) Mean duration.

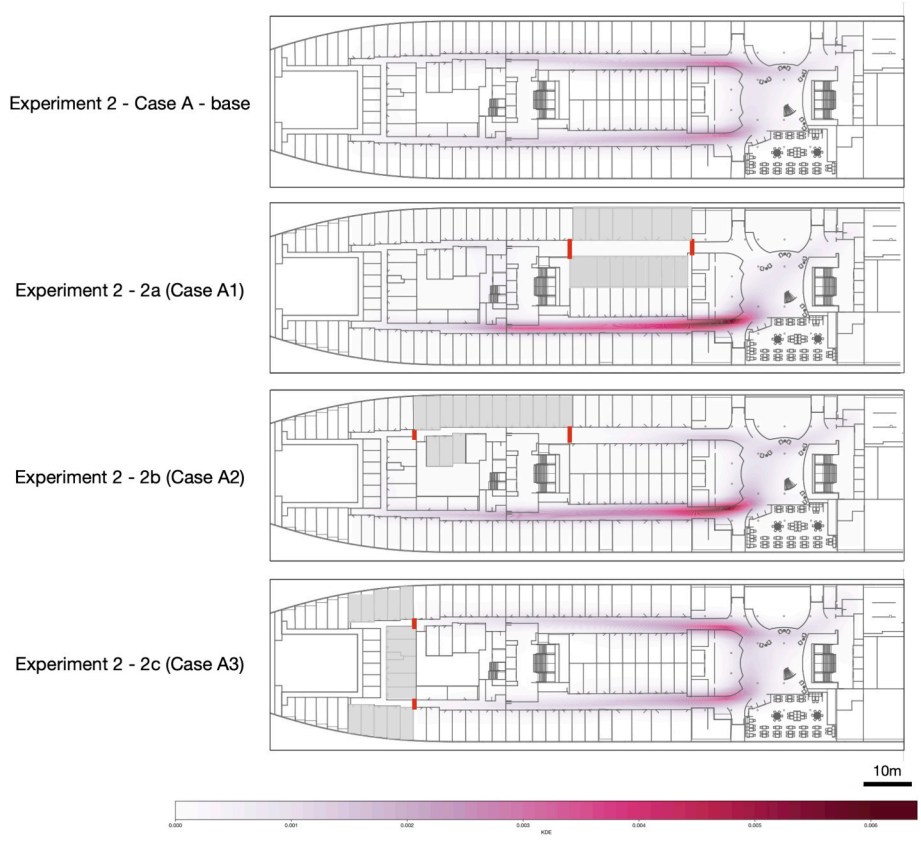

Fig. 15. Results of experiment 2: Kernel Density Estimation heat map (n = 10 in each diagram).

Table 9
Effect size (Hedge's g) of the cases in experiments 2 and 3.

Output metrics			Travel distance		Number of collisions		Travel duration	
Experiment	Control	Alternative	Hedge's g	Bias-corrected Hedge's g	Hedge's g	Bias-corrected Hedge's g	Hedge's g	Bias-corrected Hedge's g
Experiment 2	**A**	**A1**	−6.10	−5.54	−6.17	−5.61	−2.82	−2.56
	A	**A2**	0.57	0.52	−2.29	−2.08	−1.43	−1.30
	A	**A3**	5.74	5.22	0.39	0.35	1.35	1.23
Experiment 3	**C**	**C1**	−0.58	−0.52	0.61	0.55	−0.47	−0.43
	C	**C2**	−0.16	−0.15	0.60	0.55	−0.23	−0.21
	C	**C3**	−0.76	−0.69	0.57	0.52	0.03	0.03

Case C (original) yields the highest average number of collisions and the shortest average travel distance. All three design variants demonstrate a reduction in collisions, with a slight increase in travel distance. Among the alternatives, Case C2 (Perpendicular grid) achieves the lowest mean number of collisions, though with greater variability across simulations. In contrast, Case C3 (Tapering grid) exhibits more consistent performance, with lower overall range of collisions and a slightly longer average travel distance. C3 is the most connected case among all four with highest spatial connectivity (as indicated in Table 10). The Tapering grid reduces the concentration around corridors and distributes movement flows more evenly by widening the front part of the corridor. Case C1, by comparison, appears less effective, where the rear corridor is underused, limiting the benefit of added circulation space.

Modest design adjustments to internal corridor connectivity can lead to improvements in circulation and risk mitigation. The Perpendicular grid layout (C2) appears to provide the most effective balance between movement efficiency and reduced collisions, while all three variants show slight improvements over the baseline. Adding an additional corridor between two parallel corridors as an extra connection creates alternative routing options that may reduce crowd density and infection risk, albeit at the cost of some cabin spaces.

6. Discussions and conclusions

This study applies ABM to investigate how passenger movement dynamics – and, by extension, the risk of communicable disease transmission, particularly airborne pathogens are shaped by spatial configuration and operational strategies on a cruise ship deck. Through a structured set of tests and experiments, the study offers an evaluation framework and the factors influencing movement patterns.

While CFD and Wells–Riley models are valuable for estimating airborne transmission concentration and exposure (Bazant and Bush, 2021), ABM in this study is positioned as complementary to airflow-based modelling rather than as a substitute, as it captures the behavioural component of how people move, interact and crowd in a spatial layout. CFD studies on airborne transmission of infection show that ventilation and airflow influence susceptibility by altering the intensity of contaminant concentration. Using global interpersonal distance distributions as a reference, infection risk rises sharply as people move into closer proximity. At intimate distances around 0.56 m (where collision

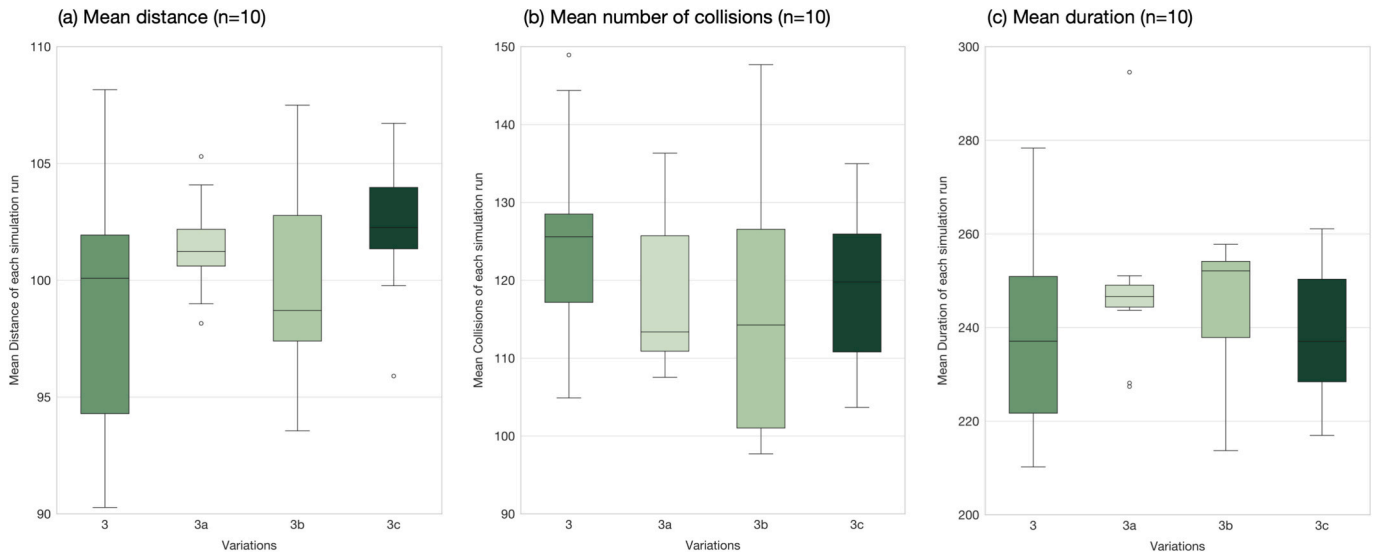

Fig. 16. Results of Experiment 3 in box plot, the average values of each simulation (n = 10): (a) Mean distance; (b) Mean number of collisions; (c) Mean duration.

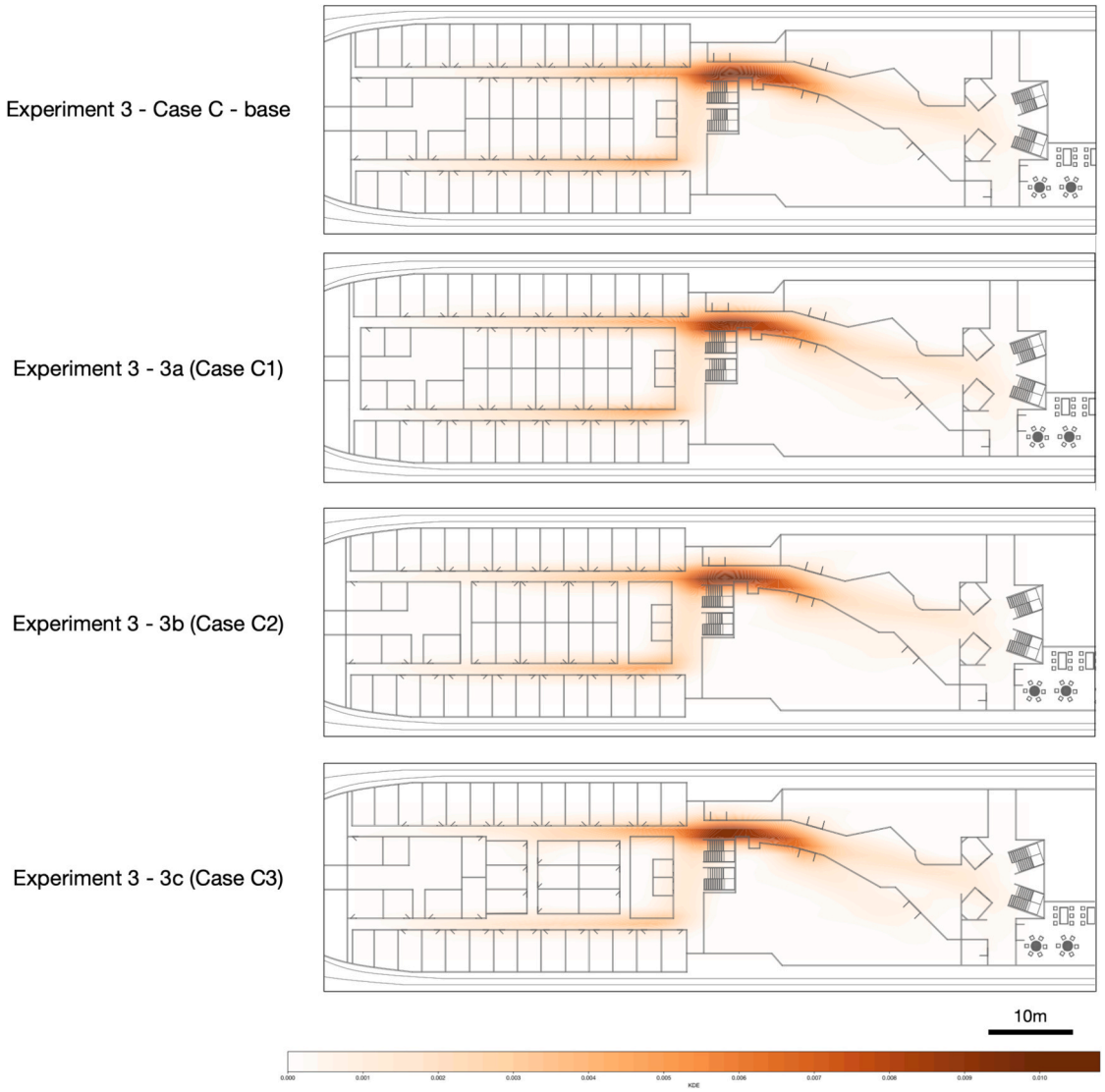

Fig. 17. Results of Experiment 3: Kernel Density Estimation heat map (n = 10 in each diagram).

Table 10
Spatial characteristics of the plans in Experiment 3.

		Experiment 3 (Case C, Parallel)	Experiment 3a (Case C1, Racetrack)	Experiment 3b (Case C2, Perpendicular grid)	Experiment 3c (Case C3, Tapering grid)
	Number of cabins	Total: 42 Inner cabin: 18 Outer cabin: 24	Total: 42 Inner cabin: 18 Outer cabin: 24	Total: 40 Inner cabin: 16 Outer cabin: 24	Total: 39 Inner cabin: 15 Outer cabin: 24
Space syntax metrics	**Connectivity**	127.606	129.371	127.31	131.953
	Isovist area	132.262	134.011	134.644	135.615
	Through vision	1153.83	1170.55	1150.02	1198.83
	Visual integration	179.567	204.735	226.782	206.431

can happen), the average risk exceeds 1 percent within only one minute of exposure, and even a ten second interaction carries a risk of about 0.2 percent (Cortellessa et al., 2021). ABM's key strength lies in its ability to simulate emergent phenomena arising from individual-level behaviours with a flexible modelling framework (Smajgl and Barreteau, 2014b), making it a powerful tool to assess system-level implications of design and operation decisions (Cotfas et al., 2023). This manuscript links spatial analysis with simulation outcomes to explain possible mobility patterns based on behavioural and spatial design.

While previous studies on cruise ship health risks have focused primarily on isolated functional spaces, such as restaurants (Triantafyllou et al., 2024a, 2024b) or cabins (Christakis and Drikakis, 2024), this study takes a more integrated approach – modelling horizontal circulation across the entire deck. This provides more holistic insights into how potential disease transmission may occur through routine movement and collisions.

Unlike evacuation-focused ABM simulations on cruise ships that typically aim to minimise evacuation time and maximise the number of evacuees (Cotfas et al., 2023; Firdhaus et al., 2023; Yue et al., 2022), this study adopts a dynamic interpretation of performance metrics instead of an absolute judgement on metrics. Travel duration and distance are not always negatively valued; longer paths may sometimes help reduce contact. However, in the context of communicable diseases transmission, the number of collisions – moments of spatial proximity between agents – serves as a risk proxy and is assumed to correlate with higher transmission potential, which would undermine health outcomes and potentially impose higher health risks for cruise ships.

This study highlights the role of design parameters in shaping human mobility in cruise ships, which is a topic that hasn't been addressed in previous research. The analysis confirms that density is a risk multiplier: denser environments lead to a significantly higher number of collisions, validated in the verification test, parametric tests (in PT1) and Experiment 1. In addition, operational interventions, such as restricting access to certain areas, can either mitigate or exacerbate crowding – depending heavily on their location and implementation strategy. The findings point to the value of a dual approach to infection mitigation: combining design-based resilience (passive control through spatial configuration and circulation networks) with operational control (active regulation of flow, density and space access).

Traditional epidemiological approaches to understanding disease transmission in confined environments are centred on contact tracing models. These models focus on person-to-person interactions, mapping social networks and tracing individual proximities and adjacencies to identify and interrupt transmission chains. While these are effective in providing insight into behavioural vectors of infection, contact tracing often abstracts away the spatial contexts in which interactions occur. Yet, spatial dynamics situates transmission not just in human networks, but within the built environment that mediates these networks. Spatial design plays a confounding role in shaping human behaviour and proxemics that influence infection dynamics. Circulation routes, spatial connectivity, ventilation pathways and enclosure geometries can either amplify or attenuate the likelihood of transmission. This study highlights the role of spatial configuration as a non-pharmaceutical, passive prevention mechanism, which remains underrepresented in public health literature. Unlike active interventions such as vaccination, testing or mask-wearing (Mosleh et al., 2024), spatial interventions work continuously through the arrangement of space that modifies exposure risk.

Summary of findings.

This study positions spatial design as an active agent in infection dynamics which could enrich epidemiological models of infection spread. By integrating spatial modelling into epidemiological simulation, we demonstrate that architectural decisions such as corridor design, location of shared amenities or strategies for zoning and quarantine can materially alter the trajectory of infection spread. We summarise key insights from the study:

- Verification tests revealed that function clustering and single-corridor layouts create flow bottlenecks. Two-corridor structures in public area (e.g. Case B), with a higher proportion of public space around the deck, are generally more effective in dispersing movement and reducing collisions. The entrance to dining spaces always tends to be the hotspots, which require further attention in order to divert the flow.
- Compact layouts (e.g. Case C) exacerbate collision risk during high-demand periods with directive walking (e.g. dining), suggesting that such layouts require complementary strategies to manage the movement flow, such as staggered access or widened corridors.
- Enforcing social distancing, modelled by increasing the agent radius to simulate avoidance behaviour, led to a reduction in collisions, but also resulted in longer travel times and distances (as shown in PT5). While such measures may lower transmission risk in principle, their real-world effectiveness would depend heavily on passenger compliance and enforcement feasibility.
- Experiment 1 confirmed a near-linear relationship between infection rates and collision frequency. As the proportion of infected agents increases, collisions involving infected individuals rise sharply, reinforcing the importance of density management as a disease control strategy.
- Experiment 2 evaluated different quarantine or hospital zone placements. It showed that the location of such zones can significantly affect circulation patterns. Poorly placed restrictions increase risk by forcing rerouting and concentrating movement elsewhere. Mid- and rear-placed zones (Cases A2 and A3) performed better than front-placed zones (A1) in terms of reducing collisions and travel disruption.
- Experiment 3 assessed design variations in cabin layouts. While the effects of these spatial reconfigurations were less pronounced than

those from operational changes, improvements were still observed. Adding a vertical corridor or widening corridors reduced collision frequency, though such interventions require trade-offs with cabin density. More creative layout strategies are needed to balance capacity and health outcomes.

Real-world implications.

While the simulations show that spatial design interventions such as widening corridors or increasing connectivity can reduce collision rates, in practice such interventions may face commercial trade-offs. Wider corridors might reduce cabin capacity and thereby impact revenue-per-square-meter, whilst retrofitting existing vessels may be difficult and expensive. Industry stakeholders could perform a cost–benefit analysis when considering layout modifications, considering both health resilience and financial viability.

The findings have direct relevance for cruise industry governance and regulation. Specifically, associations such as Cruise Lines International Association and regulatory bodies such as the International Maritime Organization may incorporate spatial-design principles (e.g. circulation connectivity, corridor width) into their health and safety guidelines. Embedding evidence-based design strategies as part of ship planning or refurbishment could form a passive, non-pharmaceutical layer of disease risk mitigation.

Limitations of the study and future research.

There are several limitations of this study. Firstly, it is essential to acknowledge that ABM is inherently stochastic and sensitive to initial conditions, though repeated simulations and verification tests were used to mitigate volatility within computational limits. Secondly, the behavioural model is relatively simple and does not yet incorporate queuing, social force, dynamic decision-making or nuanced interpersonal avoidance strategies. The simplified movement structure enables transparent sensitivity testing across architectural and operational configurations, while more detailed behavioural settings would require context-specific data to support assumptions and input data. There is a lack of empirical movement data for calibration, and only horizontal movement on a single deck was modelled – vertical circulation across between decks remains an open area for further work, as addressed in building design optimisation (Dubey et al., 2020; Gath-Morad et al., 2021). The vertical circulation spaces like staircase and elevators could also be seen as transmission hotspots that require more attention. Moreover, while collisions within 1 m serve as a useful proxy for exposure and potential transmission probability, integrating an infection transmission model would strengthen epidemiological validity (Srinivasan et al., 2024). Although 1 m is the recommendation for physical distancing for reducing COVID-19 transmission (WHO, 2025), the effective radius may vary considerably depending on pathogen-specific properties (e.g. viral load, particle size) and environmental factors such as ventilation, humidity and air currents (Scientific Advisory Group for Emergencies, 2020). Also, the case studies were informed by the project consortium and reflect realistic layouts but are not exhaustive of all possible deck configurations.

Future research could enrich the model with more detailed behavioural and environmental data, test dynamic or adaptive operational policies, simulate cross-deck movement, test different layouts for various activities and functions (such as mixed-used decks, cabin only decks and public decks), calibrate the model with empirical data and apply multi-objective optimisation techniques to evaluate trade-offs between efficiency, health safety and spatial capacity for deck plans. Ideally, future research would incorporate video-tracking or anonymised passenger mobility data to strengthen calibration and validate close-contact assumptions, to benchmark the indoor crowd movement (Zhao et al., 2021). This study provides a proof of concept of risk mapping as a parameter for infection proofing ship design. The framework could also be extended by integrating a Wells–Riley or other probabilistic infection model to more accurately represent exposure from aerosolised pathogens (Xue et al., 2024).

In addition, this study models fundamental scenarios and experiments with the quarantine intervention in a static form with fixed corridor closures, but real-world situations can be more dynamic and would require further study. Future work should consider different scenarios like trigger-based activation (e.g. upon symptom detection), zoning strategies (deck-level or corridor-level), capacity-based overflow and dedicated staff-only circulation routes. These operational extensions could more closely reflect how cruise lines respond to health emergencies in practice.

Overall, this study demonstrates that ABM can serve as a powerful tool for evidence-based design and operations planning in maritime environments and hospitality, especially in health emergencies. The findings contribute directly to the broader goal of promoting safe, healthy and resilient cruise ship travel. The approach offers a practical way to translate scientific understanding into best practices for infectious disease mitigation in the complex, high-density environments like cruise ships or hospitality environments with similar.

Declaration of generative AI and AI-assisted technologies in the writing process

During the preparation of this work the author(s) used *ChatGPT* in order to improve readability and language of the work. After using this tool/service, the author(s) reviewed and edited the content as needed and take(s) full responsibility for the content of the published article.

Data availability statement

The agent-based model simulation data that support the findings of this study is available at https://github.com/jp844/HS4U_ABM.

CRediT authorship contribution statement

Jiayu Pan: Writing – review & editing, Writing – original draft, Visualization, Software, Project administration, Methodology, Investigation, Formal analysis, Data curation, Conceptualization. **Leonel Aguilar:** Data curation. **Michal Gath-Morad:** Writing – review & editing, Methodology. **Ronita Bardhan:** Writing – review & editing, Resources, Methodology. **Koen Steemers:** Writing – review & editing, Supervision, Resources, Methodology, Funding acquisition, Conceptualization.

Declaration of competing interest

The authors declare the following financial interests/personal relationships which may be considered as potential competing interests: [Koen Steemers, Jiayu Pan, Michal Gath-Morad reports financial support was provided by UK Research and Innovation. Koen Steemers, Jiayu Pan, Michal Gath-Morad reports administrative support was provided by Horizon Europe. If there are other authors, they declare that they have no known competing financial interests or personal relationships that could have appeared to influence the work reported in this paper.].

Acknowledgements/Funding

This research is funded by the United Kingdom Research and Innovation (UKRI) (Project reference: 10051165) as part of the EU Horizon Europe-funded project 'Heathy Ship for You (HS4U)' (funded by the European Union under GA number 101069937). Views and opinions expressed are those of the author(s) only. The deck plan (Case A) was kindly provided by a project partner within the HS4U consortium.

Appendix A. Space syntax statistics

A1 Space syntax descriptives of three cases.

		Caes A	Case A (studied area)	Case B	Case C
	Count of grids	4230	2728	3508	1863
Connectivity	Average	181.59	57.38	217.99	127.61
	Min	0.00	0.00	0.00	0.00
	Max	797.00	315.00	832.00	375.00
	Std	230.04	61.31	205.93	122.79
Isovist area	Average	141.97	72.77	216.77	132.26
	Min	0.07	0.04	0.01	0.03
	Max	1230.01	1230.01	817.51	400.66
	Std	166.69	127.99	206.64	128.01
Through vision	Average	2071.95	437.20	3874.43	1153.83
	Min	9.00	0.00	0.00	0.00
	Max	19088.00	4736.00	26878.00	7189.00
	Std	4027.05	839.09	5712.87	1653.10
Visual integration	Average	16.31	19.57	7.04	179.57
	Min	1.67	1.95	1.73	2.56
	Max	780.36	780.36	96.87	2248.46
	Std	37.62	55.10	7.89	370.29

A2 Space syntax descriptives of three design alterations in Experiment 3 (EXP3).

		Whole deck				Alteration part only			
		Experiment 3 (Case C, Parallel)	Experiment 3a(Case C1, Racetrack)	Experiment 3b (Case C2, Perpendicular grid)	Experiment 3c(Case C3, Tapering grid)	Experiment 3 (Case C, Parallel)	Experiment 3a(Case C1, Racetrack)	Experiment 3b (Case C2, Perpendicular grid)	Experiment 3c(Case C3, Tapering grid)
	Count of grids	1863	1853	1849	1845	731	728	724	722
Connectivity	Average	127.61	129.37	127.31	131.95	18.52	17.78	17.73	21.47
	Min	0.00	0.00	0.00	0.00	0.00	4.00	0.00	0.00
	Max	375.00	375.00	375.00	375.00	90.00	85.00	86.00	101.00
	Std	122.79	122.79	120.61	122.76	13.67	13.14	14.32	18.64
Isovist area	Average	132.26	134.01	134.64	135.62	21.66	21.13	33.69	24.28
	Min	0.03	0.00	0.03	0.03	0.03	0.48	0.07	0.07
	Max	400.66	400.66	625.62	402.79	141.57	142.45	625.62	142.81
	Std	128.01	127.53	130.54	127.64	21.93	21.60	70.28	24.30
Through vision	Average	1153.83	1170.55	1150.02	1198.83	88.80	86.02	89.60	125.38
	Min	0.00	0.00	0.00	0.00	0.00	0.00	0.00	0.00
	Max	7189.00	7241.00	7153.00	7285.00	840.00	800.00	832.00	1040.00
	Std	1653.10	1659.28	1621.40	1671.51	195.37	188.73	192.81	253.20
Visual integration	Average	179.57	204.74	226.78	206.43	5.92	5.48	5.27	5.47
	Min	2.56	0.21	2.53	2.54	3.69	3.68	3.57	3.93
	Max	2248.46	1612.34	1570.27	1619.37	14.67	12.59	10.82	11.03
	Std	370.29	433.50	495.45	459.57	2.16	1.70	1.39	1.29

Appendix B. Verification test results

	Base case									Dinning case								
	Average value per agent in each simulation run									Average value per agent in each simulation run								
	Average distance			Average number of collisions			Average duration			Average distance			Average number of collisions			Average duration		
Case	**Case A**	**Case B**	**Case C**	**Case A**	**Case B**	**Case C**	**Case A**	**Case B**	**Case C**	**Case A**	**Case B**	**Case C**	**Case A**	**Case B**	**Case C**	**Case A**	**Case B**	**Case C**
Number of agents	100	100	100	100	100	100	100	100	100	100	100	100	100	100	100	100	100	100
Count(number of simulation runs)	50	50	50	50	50	50	50	50	50	50	50	50	50	50	50	50	50	50
Range	17.58	16.78	16.90	25.06	36.94	55.38	93.62	113.74	81.79	12.98	21.18	16.73	72.50	59.86	137.40	57.71	82.85	110.71
Mean	125.64	124.86	101.44	70.08	83.10	118.48	261.95	275.52	243.99	146.68	215.94	195.76	176.32	124.00	286.11	286.51	399.07	413.53
Standard Deviation	3.76	3.69	3.71	6.24	7.96	12.56	18.12	27.77	17.76	3.20	5.14	4.24	15.56	12.60	36.57	13.55	20.84	23.33
% (Range/Mean)	13.99 %	13.44 %	16.66 %	35.76 %	44.45 %	46.74 %	35.74 %	41.28 %	33.52 %	8.85 %	9.81 %	8.55 %	41.12 %	48.28 %	48.02 %	20.14 %	20.76 %	26.77 %
Coefficient of variation (Std/Mean)	2.99 %	2.96 %	3.66 %	8.91 %	9.57 %	10.60 %	6.92 %	10.08 %	7.28 %	2.18 %	2.38 %	2.17 %	8.82 %	10.16 %	12.78 %	4.73 %	5.22 %	5.64 %
Min	116.22	117.43	91.99	57.76	67.50	94.70	219.74	229.14	202.61	139.76	207.22	186.61	142.14	96.16	222.88	263.77	354.92	348.54
25 %	123.60	122.51	99.11	65.53	77.66	111.33	250.42	256.14	232.87	144.45	212.21	192.98	166.47	115.42	259.36	278.13	384.26	395.42
50 %	125.65	124.70	101.92	69.88	82.72	116.12	258.65	270.31	242.55	146.40	216.04	195.86	176.41	122.54	290.53	284.23	401.93	414.57
75 %	128.49	126.84	103.71	75.38	87.92	125.42	273.05	299.72	255.14	149.03	219.05	199.24	185.06	130.52	312.89	292.15	413.75	427.76
Max	133.80	134.21	108.89	82.82	104.44	150.08	313.36	342.87	284.40	152.74	228.40	203.34	214.64	156.02	360.28	321.48	437.78	459.24

Appendix C. Parametric test

Table C1 Results of PT1.

	Number of agents	Total values in each simulation run			Average per agent in each simulation run		
		Sum of distance	Total number of collisions	Sum of duration	Average distance	Average number of collisions	Average duration
Case A	100	12812.10	7422.00	28160.77	128.12	74.22	281.61
	150	19661.95	15392.00	45697.37	131.08	102.61	304.65
	200	26111.58	23944.00	69336.53	130.56	119.72	346.68
Case B	100	12805.53	9310.00	30613.70	128.06	93.10	306.14
	150	20007.80	22236.00	53091.59	133.39	148.24	353.94
	200	27692.14	39830.00	84477.40	138.46	199.15	422.39
Case C	100	9908.57	11060.00	23118.18	99.09	110.60	231.18
	150	17136.48	32294.00	41057.71	114.24	215.29	273.72
	200	23009.44	48876.00	64246.05	115.05	244.38	321.23

Table C2 Results of PT2 to PT 7.

Parameter		Case A			Case B			Case C		
		Average distance	Average number of collisions	Average duration	Average distance	Average number of collisions	Average duration	Average distance	Average number of collisions	Average duration
PT2 Spawn interval	1	128.73	72.28	291.89	124.25	92.12	282.37	97.47	108.36	236.15
	2	122.50	42.72	277.88	127.03	76.62	322.25	101.16	82.80	268.72
	3	124.92	35.62	321.97	126.12	50.70	365.23	92.66	44.80	303.43
	4	116.97	23.36	371.63	125.75	48.42	402.38	91.70	34.40	339.14
	5	119.99	21.70	412.14	125.49	29.60	404.12	96.18	31.60	378.97
PT3 Number of needs	1	121.34	80.18	280.95	126.24	83.64	260.94	102.84	124.86	275.65
	2	140.47	78.98	297.76	145.10	68.78	298.25	122.49	140.80	278.25
	3	160.51	115.90	330.76	164.97	80.44	278.62	139.20	124.60	300.74
	4	172.00	117.80	342.67	181.98	92.64	305.05	163.43	167.52	376.73
	5	190.17	203.58	413.09	214.17	114.66	393.75	196.85	242.56	387.30
PT4 Agent size	0.6	122.90	71.72	244.99	121.59	89.28	228.47	95.24	109.60	225.53
	0.7	118.53	70.18	240.32	123.44	88.86	270.29	101.92	141.60	216.70
	0.8	127.77	77.54	235.29	126.25	83.72	327.10	100.58	129.24	256.96
	0.9	122.55	55.60	293.89	128.21	73.52	296.42	101.44	114.58	232.19
	1	131.55	30.56	246.37	129.75	46.38	274.62	107.37	72.10	265.91
PT5 Agent radius	0.1	114.70	54.14	211.96	110.19	78.80	223.34	85.61	84.76	172.18
	0.2	118.17	71.23	226.52	117.46	84.18	237.70	81.38	76.90	190.92
	0.3	122.60	76.88	255.72	114.04	86.24	216.47	90.32	113.94	209.35
	0.4	122.18	73.90	259.29	122.37	98.40	245.70	98.87	123.84	192.24
	0.5	121.81	67.56	272.92	125.50	95.82	280.76	101.30	112.36	233.70
	0.6	131.10	49.26	263.09	136.22	74.70	293.55	106.59	88.52	248.84
	0.7	132.51	11.94	266.85	134.70	20.28	297.85	133.40	54.00	328.58
	0.8	138.88	7.72	268.94	148.48	23.26	380.14	135.92	65.42	350.87
	0.9	151.94	16.28	379.37	154.99	27.74	323.39	159.87	55.84	395.02
	1.0	157.63	14.96	329.11	166.44	30.30	386.38	195.30	77.46	531.11
PT6 Privacy radius	0.5	119.00	0.92	244.65	122.58	1.18	286.82	95.93	3.10	225.95
	0.6	126.70	2.82	278.87	119.30	1.24	260.41	104.35	6.22	252.74
	0.7	120.98	1.96	261.90	127.00	4.32	276.89	102.63	7.84	260.13
	0.8	124.81	27.94	260.41	121.71	29.20	253.23	98.87	45.18	224.13
	0.9	124.81	41.64	254.23	126.82	63.88	285.72	102.01	112.24	245.93
	1.0	124.41	64.20	243.19	127.13	92.20	291.50	96.99	115.06	246.55
	1.1	122.57	91.30	255.97	128.27	108.22	279.51	100.34	153.62	227.75
	1.2	125.43	114.26	236.71	122.85	164.56	330.94	103.79	185.08	251.34
	1.3	130.18	115.14	237.76	124.18	155.52	259.84	99.29	180.10	253.01
	1.4	127.51	156.60	255.15	126.38	148.42	269.09	102.66	248.96	248.46
	1.5	122.75	159.88	236.72	123.10	193.72	337.15	102.27	235.66	234.05
	1.6	124.23	165.18	268.28	129.59	214.30	302.78	103.61	286.06	273.08
	1.7	120.59	172.24	265.55	131.69	225.34	303.67	97.68	289.94	217.02
	1.8	117.77	182.84	235.43	118.70	224.36	294.45	104.78	384.02	263.35
	1.9	123.20	208.40	254.92	129.55	275.90	266.68	105.12	398.68	232.95
	2.0	129.36	282.74	226.33	122.55	272.61	308.99	95.40	367.73	248.72
PT7 POI Time	1	126.71	67.88	261.45	124.39	89.23	345.93	104.70	130.70	257.92

(continued on next page)

(*continued*)

Parameter		Case A Average distance	Average number of collisions	Average duration	Case B Average distance	Average number of collisions	Average duration	Case C Average distance	Average number of collisions	Average duration
	2	116.06	67.22	245.53	123.53	81.66	245.03	104.45	134.48	231.97
	3	128.29	67.80	260.50	131.69	90.22	323.15	103.28	129.28	248.91
	4	121.90	75.66	255.62	125.47	100.69	300.39	95.75	106.30	219.16
	5	126.93	87.70	267.41	123.32	79.66	311.48	103.94	137.16	255.70

Appendix D. Results of experiments 2 and 3

Experiment	Deck plan	Count(number of simulations)	Average value per agent in each simulation run: Average distance Mean	Std	Average number of collisions Mean	Std	Average duration Mean	Std
Experiment 2	Case A	10	124.53	2.62	71.60	6.22	245.92	14.87
Experiment 2a	Case A1	10	151.51	5.68	141.82	14.84	290.73	16.87
Experiment 2b	Case A2	10	122.69	3.74	89.38	9.03	280.24	30.42
Experiment 2c	Case A3	10	108.08	3.09	68.98	7.32	225.32	15.67
Experiment 3	Case C	10	99.00	5.59	125.10	13.95	238.96	21.34
Experiment 3a	Case C1, Racetrack	10	101.45	2.14	117.75	9.99	248.26	18.32
Experiment 3b	Case C2, Perpendicular grid	10	99.82	4.43	115.86	16.54	243.40	16.53
Experiment 3c	Case C3,Tapering grid	10	102.43	3.17	118.12	10.37	238.35	16.03

.

References

Anagnostopoulos, L., Vasileiadis, S., Kourentis, L., Bogogiannidou, Z., Voulgaridi, I., Nichols, G., Kalala, F., Speletas, M., Hadjichristodoulou, C., Mouchtouri, V.A., the EU HEALTHY SAILING project, Amditis, A., Athanasiadis, S., Bansaghi, S.J., Bygvraa, D. A., Chatzimichelakis, S., D'Souza, R., Dionysiou, D., Guerrero-Vadillo, M., Guzzetta, G., Harth, V., Heidrich, J., Klein, J., Kolb, J.F., Kumar, P., Lepore, P., Lupu, S., Marziano, V., Neumann, J., Nikolaou, S., Nistor, F., Ouzounoglou, E., Papataxiarhis, V., Peñuelas, M., Pezzotti, P., Popa, C., Rataj, R., Reppa, S., Riccardo, F., Salmela, H., Siilin, N., Theofilis, K., Tsibanis, C., Varela, C., Ventikos, N.P., Vosinakis, G., Vukelić, G., Zädow, C., Zagkas, V., 2025. Scoping review of infectious disease prevention, mitigation and management in passenger ships and at ports: mapping the literature to develop comprehensive and effective public health measures. Trop. Med. Health 53, 3. https://doi.org/10.1186/s41182-025-00681-0.

Antczak, T., Skorupa, B., Szurlej, M., Weron, R., Zabawa, J., 2021. Simulation Modeling of Epidemic Risk in Supermarkets: Investigating the Impact of Social Distancing and Checkout Zone Design, in: Paszynski, M., Kranzlmüller, D., Krzhizhanovskaya, V.V., Dongarra, J.J., Sloot, P.M.A. (Eds.), Computational Science – ICCS 2021, Lecture Notes in Computer Science. Springer International Publishing, Cham, pp. 26–33. https://doi.org/10.1007/978-3-030-77961-0_3.

Arup, 2024. MassMotion [WWW Document]. Arup Digit. Solut. Tools. URL https://www.arup.com/services/digital-solutions-and-tools/massmotion/.

Azimi, P., Keshavarz, Z., Cedeno Laurent, J.G., Stephens, B., Allen, J.G., 2021. Mechanistic transmission modeling of COVID-19 on the *Diamond Princess* cruise ship demonstrates the importance of aerosol transmission. Proc. Natl. Acad. Sci. 118, e2015482118. https://doi.org/10.1073/pnas.2015482118.

Baraniuk, C., 2020. What the Diamond Princess taught the world about covid-19. BMJ m1632. https://doi.org/10.1136/bmj.m1632.

Bardhan, R., Debnath, R., Malik, J., Sarkar, A., 2018. Low-income housing layouts under socio-architectural complexities: a parametric study for sustainable slum rehabilitation. Sustain. Cities Soc. 41, 126–138. https://doi.org/10.1016/j.scs.2018.04.038.

Bardhan, R., Pan, J., Chen, S., Cho, T.Y., 2024. Breathing space in a compact city: impacts of urban re-densification on Mumbai's low-income housing environment. Habitat Int. 149, 103098. https://doi.org/10.1016/j.habitatint.2024.103098.

Baur, R., Gath-Morad, M., Hölscher, C., 2023. DesignMind Toolkit. https://doi.org/10.5281/ZENODO.7791793.

Bazant, M.Z., Bush, J.W.M., 2021. A guideline to limit indoor airborne transmission of COVID-19. Proc. Natl. Acad. Sci. 118, e2018995118. https://doi.org/10.1073/pnas.2018995118.

Benedikt, M.L., 1979. To take hold of space: isovists and isovist fields. Environ. Plan. B Plan. Des. 6, 47–65. https://doi.org/10.1068/b060047.

Bert, F., Scaioli, G., Gualano, M.R., Passi, S., Specchia, M.L., Cadeddu, C., Viglianchino, C., Siliquini, R., 2014. Norovirus outbreaks on commercial cruise ships: a systematic review and new targets for the public health agenda. Food Environ. Virol. 6, 67–74. https://doi.org/10.1007/s12560-014-9145-5.

Bonabeau, E., 2002. Agent-based modeling: methods and techniques for simulating human systems. Proc. Natl. Acad. Sci. 99, 7280–7287. https://doi.org/10.1073/pnas.082080899.

Castillo-Manzano, J.I., López-Valpuesta, L., 2018. What does cruise passengers' satisfaction depend on? does size really matter? Int. J. Hosp. Manag. 75, 116–118. https://doi.org/10.1016/j.ijhm.2018.03.013.

Castle, C.J.E., Waterson, N.P., Pellissier, E., Le Bail, S., 2011. A Comparison of Grid-based and Continuous Space Pedestrian Modelling Software: Analysis of Two UK Train Stations, in: Peacock, R.D., Kuligowski, E.D., Averill, J.D. (Eds.), Pedestrian and Evacuation Dynamics. Springer US, Boston, MA, pp. 433–446. https://doi.org/10.1007/978-1-4419-9725-8_39.

Cheliotis, K., 2021. ABMU: an agent-based modelling framework for Unity3D. SoftwareX 15, 100771. https://doi.org/10.1016/j.softx.2021.100771.

Cheliotis, K., 2020. An agent-based model of public space use. Comput. Environ. Urban Syst. 81, 101476. https://doi.org/10.1016/j.compenvurbsys.2020.101476.

Christakis, N., Drikakis, D., 2024. On particle dispersion statistics using unsupervised learning and Gaussian mixture models. Phys. Fluids 36, 093317. https://doi.org/10.1063/5.0229111.

Chu, D.K., Akl, E.A., Duda, S., Solo, K., Yaacoub, S., Schünemann, H.J., Chu, D.K., Akl, E. A., El-harakeh, A., Bognanni, A., Lotfi, T., Loeb, M., Hajizadeh, A., Bak, A., Izcovich, A., Cuello-Garcia, C.A., Chen, C., Harris, D.J., Borowiack, E., Chamseddine, F., Schünemann, F., Morgano, G.P., Muti Schünemann, G.E.U., Chen, G., Zhao, H., Neumann, I., Chan, J., Khabsa, J., Hneiny, L., Harrison, L., Smith, M., Rizk, N., Giorgi Rossi, P., AbiHanna, P., El-khoury, R., Stalteri, R., Baldeh, T., Piggott, T., Zhang, Y., Saad, Z., Khamis, A., Reinap, M., Duda, S., Solo, K., Yaacoub, S., Schünemann, H.J., 2020. Physical distancing, face masks, and eye protection to prevent person-to-person transmission of SARS-CoV-2 and COVID-19: a systematic review and meta-analysis. Lancet 395, 1973–1987. https://doi.org/10.1016/S0140-6736(20)31142-9.

Clements, N., Binnicker, M.J., Roger, V.L., 2020. Indoor environment and viral infections. Mayo Clin. Proc. 95, 1581–1583. https://doi.org/10.1016/j.mayocp.2020.05.028.

Codreanu, T.A., Ngeh, S., Trewin, A., Armstrong, P.K., 2021. Successful control of an onboard COVID-19 outbreak using the cruise ship as a quarantine facility, Western Australia. Australia. Emerg. Infect. Dis. 27, 1279–1287. https://doi.org/10.3201/eid2705.204142.

CORDIS, 2022. Healthy Ship 4U. CORDIS - EU Res. Results HORIZON-RIA-HORIZON Research and Innovation Actions. https://doi.org/10.3030/101069937.

Cortellessa, G., Stabile, L., Arpino, F., Faleiros, D.E., Van Den Bos, W., Morawska, L., Buonanno, G., 2021. Close proximity risk assessment for SARS-CoV-2 infection. Sci. Total Environ. 794, 148749. https://doi.org/10.1016/j.scitotenv.2021.148749.

Cotfas, L.-A., Delcea, C., Mancini, S., Ponsiglione, C., Vitiello, L., 2023. An agent-based model for cruise ship evacuation considering the presence of smart technologies on board. Expert Syst. Appl. 214, 119124. https://doi.org/10.1016/j.eswa.2022.119124.

Cruise Lines International Association, 2024. Contribution of Cruise Tourism to the Global Economy 2023 (Economic Impact Studies). Cruise Lines International Association.

CruiseMapper services, 2024. CruiseMapper [WWW Document]. CruiseMapper. URL https://www.cruisemapper.com/.

D'Orazio, M., Bernardini, G., Quagliarini, E., 2021. A probabilistic model to evaluate the effectiveness of main solutions to COVID-19 spreading in university buildings according to proximity and time-based consolidated criteria. Build. Simul. 14, 1795–1809. https://doi.org/10.1007/s12273-021-0770-2.

Dubey, R.K., Khoo, W.P., Morad, M.G., Hölscher, C., Kapadia, M., 2020. AUTOSIGN: a multi-criteria optimization approach to computer aided design of signage layouts in complex buildings. Comput. Graph. 88, 13–23. https://doi.org/10.1016/j.cag.2020.02.007.

Ekholm, A., 2001. Modelling of User Activities in Building Design. Presented at the eCAADe 2001: Architectural information management, Helsinki, Finland, pp. 67–72. https://doi.org/10.52842/conf.ecaade.2001.067.

Firdhaus, A., Mulyatno, I.P., Hakim, M.L., Zen, Z., 2023. Passengers and Crew's Evacuation from passenger ships under fire: an agent-based model simulation study. Kapal J. Ilmu Pengetah. Dan Teknol. Kelaut. 20, 85–91. https://doi.org/10.14710/kapal.v20i1.50714.

Gath-Morad, M., Baur, R., Hölscher, C., 2023. The DesignMind toolkit. Presented at the eCAADe 2023: Digital Design Reconsidered, Graz, Austria, pp. 51–60. https://doi.org/10.52842/conf.ecaade.2023.1.051.

Gath-Morad, M., Thrash, T., Schicker, J., Hölscher, C., Helbing, D., Aguilar Melgar, L.E., 2021. Visibility matters during wayfinding in the vertical. Sci. Rep. 11, 18980. https://doi.org/10.1038/s41598-021-98439-1.

Gath-Morad, M., Zinger, E., Schaumann, D., Pilosof, N.P., Kalay, Y.E., 2018. A Dashboard Model to Support Spatio-Temporal Analysis of Simulated Human Behavior in Future Built Environments. Presented at the SimAUD 2017, Society for Modeling & Simulation International (SCS), Toronto, Canada.

Golna, C., Markakis, I.A., Tzavara, C., Golnas, P., Ntokou, A., Souliotis, K., 2024. Screening and early detection of communicable diseases on board cruise ships: an assessment of passengers' preferences on technical solutions. Travel Med. Infect. Dis. 60, 102729. https://doi.org/10.1016/j.tmaid.2024.102729.

Hao, J., 2023. Research on the early warning and prevention system of infectious diseases based on large cruise ships. Highlights Sci. Eng. Technol. 56, 392–398. https://doi.org/10.54097/hset.v56i.10700.

Hillier, B., Hanson, J., 1984. The Social Logic of Space, 1st ed. Cambridge University Press. https://doi.org/10.1017/CBO9780511597237.

Hong, S.W., Schaumann, D., Kalay, Y.E., 2016. Human behavior simulation in architectural design projects: an observational study in an academic course. Comput. Environ. Urban Syst. 60, 1–11. https://doi.org/10.1016/j.compenvurbsys.2016.07.005.

Huang, L.-S., Li, L., Dunn, L., He, M., 2021. Taking account of asymptomatic infections: a modeling study of the COVID-19 outbreak on the Diamond Princess cruise ship. PLoS One 16, e0248273. https://doi.org/10.1371/journal.pone.0248273.

Japan Institute for Health Security, 2020. Field Briefing: Diamond Princess COVID-19 Cases [WWW Document]. Infect. Dis. Inf. Website. URL https://id-info.jihs.go.jp/niid/en/2019-ncov-e/9407-covid-dp-fe-01.html (accessed 5.22.25).

Jia, Z., Nourian, P., Luscuere, P., Wagenaar, C., 2023. Spatial decision support systems for hospital layout design: a review. J. Build. Eng. 67, 106042. https://doi.org/10.1016/j.jobe.2023.106042.

J.P. Morgan Research, 2024. Is the outlook for the cruise industry plain sailing? [WWW Document]. Glob. Res. URL https://www.jpmorgan.com/insights/global-research/travel/cruise-outlook (accessed 1.20.25).

Kasereka, S., Kasoro, N., Kyamakya, K., Doungmo Goufo, E.-F., Chokki, A.P., Yengo, M. V., 2018. Agent-based modelling and simulation for evacuation of people from a building in case of fire. Procedia Comput. Sci. 130, 10–17. https://doi.org/10.1016/j.procs.2018.04.006.

Li, Z., Shao, W.B., 2021. Research on cruise space planning and design based on spatial syntax and correlation analysis. Proceedings in Marine Technology and Ocean Engineering. Presented at the MARTECH. CRC Press, Boca Raton London New York.

Liu, S., Lo, S., Ma, J., Wang, W., 2014. An agent-based microscopic pedestrian flow simulation model for pedestrian traffic problems. IEEE Trans. Intell. Transp. Syst. 15, 992–1001. https://doi.org/10.1109/TITS.2013.2292526.

Martinez, I., Bruse, J.L., Florez-Tapia, A.M., Viles, E., Olaizola, I.G., 2022. ArchABM: an agent-based simulator of human interaction with the built environment. CO2 and viral load analysis for indoor air quality. Build. Environ. 207, 108495. https://doi.org/10.1016/j.buildenv.2021.108495.

McNeel, R., 2024. Rhinoceros 3D.

Mohamadi, F., Fazeli, A., 2022. A review on applications of CFD modeling in COVID-19 pandemic. Arch. Comput. Meth. Eng. 29, 3567–3586. https://doi.org/10.1007/s11831-021-09706-3.

Moloney, M.J., 2018. Re-imagining shipboard societies: a spatial approach to analysing ships of the British Royal Navy during the eighteenth and nineteenth centuries. Int. J. Marit. Hist. 30, 315–342. https://doi.org/10.1177/0843871418766766.

Morad, M., Aguilar, L., Dalton, R., Hölscher, C., 2020. cogARCH: Simulating wayfinding by architecture in multilevel buildings.

Mosleh, R., Baky-Haskuee, M., Ghasemi, A., Grunnill, M., Arino, J., Tofighi, M., Thommes, E.W., Wu, J., 2024. Evaluating infectious disease outbreak potential and mitigation effectiveness on cruise ships. J. Theor. Biol. 592, 111875. https://doi.org/10.1016/j.jtbi.2024.111875.

Nemhauser, J.B., Centers for Disease Control (U.S.) (Eds.), 2023. CDC yellow book 2024: health information for international travel. Oxford University Press, New York, NY. https://doi.org/10.1093/oso/9780197570944.001.0001.

Neufert, E., Neufert, P., Kister, J., 2012. Architects' data, 4th ed. ed. Wiley-Blackwell, Chichester, West Sussex, UK ; Ames, Iow.

Neumayr, R.R., 2019. Simulation tools for social performance, in: Kanaani, M. (Ed.), The Routledge Companion to Paradigms of Performativity in Design and Architecture. Routledge, pp. 287–300. https://doi.org/10.4324/9780429021640-26.

Noakes, C.J., Beggs, C.B., Sleigh, P.A., Kerr, K.G., 2006. Modelling the transmission of airborne infections in enclosed spaces. Epidemiol. Infect. 134, 1082–1091. https://doi.org/10.1017/S0950268806005875.

Noyman, A., Hu, K., Larson, K., 2024. TravelAgent: generative agents in the built environment. ArXiv Prepr.

Ozturk, U.A., Gogtas, H., 2016. Destination attributes, satisfaction, and the cruise visitor's intent to revisit and recommend. Tour. Geogr. 18, 194–212. https://doi.org/10.1080/14616688.2015.1124446.

Pan, J., Cho, T.Y., Bardhan, R., 2021. Redesigning the working space for social distancing: modelling the movement in an open-plan office. Presented at the CIBSE Technical Symposiu.

Ren, C., Yang, C., Jin, S., 2009. Agent-based modeling and simulation on emergency evacuation, in: Zhou, J. (Ed.), Complex Sciences, Lecture Notes of the Institute for Computer Sciences, Social Informatics and Telecommunications Engineering. Springer Berlin Heidelberg, Berlin, Heidelberg, pp. 1451–1461. https://doi.org/10.1007/978-3-642-02469-6_25.

Rocklöv, J., Sjödin, H., Wilder-Smith, A., 2020. COVID-19 outbreak on the Diamond Princess cruise ship: estimating the epidemic potential and effectiveness of public health countermeasures. J. Travel Med. 27, taaa030. https://doi.org/10.1093/jtm/taaa030.

Salgado, M., Gilbert, N., 2013. Agent based modelling, in: Teo, T. (Ed.), Handbook of Quantitative Methods for Educational Research. SensePublishers, Rotterdam, pp. 247–265. https://doi.org/10.1007/978-94-6209-404-8_12.

Schaumann, D., Breslav, S., Goldstein, R., Khan, A., Kalay, Y.E., 2017. Simulating use scenarios in hospitals using multi-agent narratives. J. Build. Perform. Simul. 10, 636–652. https://doi.org/10.1080/19401493.2017.1332687.

Schaumann, D., Moon, S., Usman, M., Goldstein, R., Breslav, S., Khan, A., Faloutsos, P., Kapadia, M., 2020. JOIN: an integrated platform for joint simulation of occupant-building interactions. Archit. Sci. Rev. 63, 339–350. https://doi.org/10.1080/00038628.2019.1662767.

Scientific Advisory Group for Emergencies, 2020. Environmental influence on transmission of COVID-19 (Research and analysis), Health and social care COVID-19. GOV.UK.

Shirreff, G., Thiébaut, A.C.M., Huynh, B.-T., Chelius, G., Fraboulet, A., Guillemot, D., Opatowski, L., Temime, L., 2024. Hospital population density and risk of respiratory infection: is close contact density dependent? Epidemics 49, 100807. https://doi.org/10.1016/j.epidem.2024.100807.

Silverman, B.W., 1998. Density estimation for statistics and data analysis, Monographs on statistics and applied probability. Chapman & Hall/CRC, Boca Raton.

Smajgl, A., Barreteau, O., 2014a. Empirical agent-based modelling - challenges and solutions. Springer, New York Heidelberg.

Smajgl, A., Barreteau, O., 2014b. Empiricism and agent-based modelling. In: Smajgl, A., Barreteau, O. (Eds.), Empirical Agent-Based Modelling - Challenges and Solutions. Springer, New York, New York, NY, pp. 1–26. https://doi.org/10.1007/978-1-4614-6134-0_1.

Sofos, F., Drikakis, D., Kokkinakis, I.W., 2025. Enhancing indoor temperature mapping: high-resolution insights through deep learning and computational fluid dynamics. Phys. Fluids 37, 015206. https://doi.org/10.1063/5.0250478.

Sovatzidi, G., Triantafyllou, G., Dimas, G., Kalozoumis, P.G., Drikakis, D., Kokkinakis, I. W., Markakis, I.A., Golna, C., Iakovidis, D.K., 2024. Risk Assessment of COVID-19 Transmission on Cruise Ships Using Fuzzy Rules, in: Maglogiannis, I., Iliadis, L., Macintyre, J., Avlonitis, M., Papaleonidas, A. (Eds.), Artificial Intelligence Applications and Innovations, IFIP Advances in Information and Communication Technology. Springer Nature Switzerland, Cham, pp. 336–348. https://doi.org/10.1007/978-3-031-63219-8_25.

Srinivasan, S., King, J., Colubri, A., Korkin, D., 2024. Real-time spatiotemporal tracking of infectious outbreaks in confined environments with a host-pathogen agent-based system. BioRxiv Prepr. Serv. Biol. https://doi.org/10.1101/2024.10.01.616085.

Stieler, D., Schwinn, T., Leder, S., Maierhofer, M., Kannenberg, F., Menges, A., 2022. Agent-based modeling and simulation in architecture. Autom. Constr. 141, 104426. https://doi.org/10.1016/j.autcon.2022.104426.

Tabak, V., De Vries, B., Dijkstra, J., 2010. Simulation and validation of human movement in building spaces. Environ. Plan. B Plan. Des. 37, 592–609. https://doi.org/10.1068/b35127.

Toroczkai, Z., Guclu, H., 2007. Proximity networks and epidemics. Phys. Stat. Mech. Its Appl. 378, 68–75. https://doi.org/10.1016/j.physa.2006.11.088.

Torrens, P.M., 2015. Intertwining agents and environments. Environ. Earth Sci. 74, 7117–7131. https://doi.org/10.1007/s12665-015-4738-3.

Torrens, P.M., 2012. Moving agent pedestrians through space and time. Ann. Assoc. Am. Geogr. 102, 35–66. https://doi.org/10.1080/00045608.2011.595658.

Triantafyllou, G., Kalozoumis, P.G., Cholopoulou, E., Iakovidis, D.K., 2024a. In: Disease Spread Control in Cruise Ships: Monitoring, Simulation, and Decision Making. The Blue Book. Springer International Publishing, Cham, pp. 93–141. https://doi.org/10.1007/978-3-031-48831-3_8.

Triantafyllou, G., Sovatzidi, G., Dimas, G., Kalozoumis, P.G., Drikakis, D., Kokkinakis, I. W., Markakis, I.A., Golna, C., Iakovidis, D., 2024b. Sensor-based fuzzy inference of COVID-19 transmission risk in cruise ships. In: Mantas, J., Hasman, A., Demiris, G., Saranto, K., Marschollek, M., Arvanitis, T.N., Ognjanović, I., Benis, A., Gallos, P., Zoulias, E., Andrikopoulou, E. (Eds.), Studies in Health Technology and Informatics. IOS Press. https://doi.org/10.3233/SHTI240784.

Turner, A., Doxa, M., O'Sullivan, D., Penn, A., 2001. From Isovists to visibility graphs: a methodology for the analysis of architectural space. Environ. Plan. B Plan. Des. 28, 103–121. https://doi.org/10.1068/b2684.

UCL Space Syntax, 2024. Space Syntax Glossary [WWW Document]. Space Syntax Online Train. Platf. URL https://www.spacesyntax.online/glossary/.

Unity Technologies, 2024. Unity.

Wang, Z., Galea, E.R., Grandison, A., Ewer, J., Jia, F., 2022. A coupled computational fluid dynamics and wells-riley model to predict COVID-19 infection probability for passengers on long-distance trains. Saf. Sci. 147, 105572. https://doi.org/10.1016/j.ssci.2021.105572.

Wang, Z., Zhu, Y., Li, K., Cheng, J., Xing, L., 2023. Suggestions on Health and Safety Measures and Epidemic Prevention and Control Measures on Luxury Cruise Ships. World J. Public Health. https://doi.org/10.11648/j.wjph.20230802.20.

WHO, 2025. COVID-19: physical distancing [WWW Document]. World Health Organ. URL https://www.who.int/westernpacific/emergencies/covid-19/information/physical-distancing (accessed 11.16.25).

Wurzer, G., Popov, N., Lorenz, W., 2012. Meeting simulation needs of early-stage design through agent-based simulation. Presented at the eCAADe 2012 : Digital Physicality, Prague, Czech Republic, pp. 613–620. https://doi.org/10.52842/conf.ecaade.2012.1.613.

Xia, Z., Guan, H., Qi, Z., Xu, P., 2023. Multi-zone infection risk assessment model of airborne virus transmission on a cruise ship using CONTAM. Buildings 13, 2350. https://doi.org/10.3390/buildings13092350.

Xie (Jimmy), H., Kerstetter, D.L., Mattila, A.S., 2012. The attributes of a cruise ship that influence the decision making of cruisers and potential cruisers. Int. J. Hosp. Manag. 31, 152–159. https://doi.org/10.1016/j.ijhm.2011.03.007.

Xu, Q., Chraibi, M., 2020. On the effectiveness of the measures in supermarkets for reducing contact among customers during COVID-19 period. Sustainability 12, 9385. https://doi.org/10.3390/su12229385.

Xue, Y., Jabi, W., Woolley, T.E., Kaouri, K., 2024. Modelling indoor airborne transmission combining architectural design and people movement using the VIRIS simulator and web app. Sci. Rep. 14, 28220. https://doi.org/10.1038/s41598-024-79525-6.

Yamamura, O., Onishi, H., Sakamaki, I., Fujita, R., Miyashita, H., Iwasaki, H., 2023. Infection rate among close contacts of patients with coronavirus disease in Japan: a descriptive study and literature review. Asian Biomed. 17, 115–123. https://doi.org/10.2478/abm-2023-0051.

Yan, D., O'Brien, W., Hong, T., Feng, X., Burak Gunay, H., Tahmasebi, F., Mahdavi, A., 2015. Occupant behavior modeling for building performance simulation: current state and future challenges. Energ. Buildings 107, 264–278. https://doi.org/10.1016/j.enbuild.2015.08.032.

Yu, S., 2023. Evaluating architectural layouts for occupancy patterns and interactions using agent-based modelling as a methodology for workplace design. Autom. Constr. 155, 105025. https://doi.org/10.1016/j.autcon.2023.105025.

Yu, S., 2022. Agent-based modelling using survey data to simulate occupancy patterns and occupant interactions for workplace design. Build. Environ. 224, 109519. https://doi.org/10.1016/j.buildenv.2022.109519.

Yue, Y., Gai, W., Deng, Y., 2022. Influence factors on the passenger evacuation capacity of cruise ships: modeling and simulation of full-scale evacuation incorporating information dissemination. Process Saf. Environ. Prot. 157, 466–483. https://doi.org/10.1016/j.psep.2021.11.010.

Yuen, K.F., Bin Saidi, M.S., Bai, X., Wang, X., 2021. Cruise transport service usage post COVID-19: the health belief model application. Transp. Policy 111, 185–196. https://doi.org/10.1016/j.tranpol.2021.08.002.

Zhang, L., 2024. Exploring pathogen population density as a metric for understanding post-COVID infectious disease surges. Front. Immunol. 15, 1459628. https://doi.org/10.3389/fimmu.2024.1459628.

Zhang, N., Miao, R., Huang, H., Chan, E.Y.Y., 2016. Contact infection of infectious disease onboard a cruise ship. Sci. Rep. 6, 38790. https://doi.org/10.1038/srep38790.

Zhang, S., Diao, M., Yu, W., Pei, L., Lin, Z., Chen, D., 2020. Estimation of the reproductive number of novel coronavirus (COVID-19) and the probable outbreak size on the Diamond Princess cruise ship: a data-driven analysis. Int. J. Infect. Dis. 93, 201–204. https://doi.org/10.1016/j.ijid.2020.02.033.

Zhao, Y., Zhao, X., Chen, S., Zhang, Z., Huang, X., 2021. An indoor crowd movement trajectory benchmark dataset. IEEE Trans. Reliab. 70, 1368–1380. https://doi.org/10.1109/TR.2021.3109122.

Zhen, Q., Zhang, A., Huang, Q., Li, J., Du, Y., Zhang, Q., 2022. Overview of the role of spatial factors in indoor SARS-CoV-2 transmission: a space-based framework for assessing the multi-route infection risk. Int. J. Environ. Res. Public Health 19, 11007. https://doi.org/10.3390/ijerph191711007.

Zhou, J., Koutsopoulos, H.N., 2021. Virus Transmission risk in urban rail systems: microscopic simulation-based analysis of spatio-temporal characteristics. Transp. Res. Rec. J. Transp. Res. Board 2675, 120–132. https://doi.org/10.1177/03611981211010181.